Physics – Uspekhi **39** (8) 759 – 780 (1996)

REVIEWS OF TOPICAL PROBLEMS PACS numbers: 97.60.Lf, **97.80.–d**

Masses of black holes in binary stellar systems

A M Cherepashchuk

Contents

Abstract. Mass determination methods and their results for ten black holes in X-ray binary systems are summarised. A unified interpretation of the radial velocity and optical light curves allows one to reliably justify the close binary system model and to prove the correctness of determination of the optical star mass function $f_v(m)$. The orbit plane inclination i can be estimated from an analysis of optical light curve of the system, which is due mainly to the ellipsoidal shape of the optical star (the so-called ellipticity effect). The component mass ratio $q = m_x/m_v$ is obtained from information about the distance to the binary system as well as from data about rotational broadening of absorption lines in the spectrum of the optical star. These data allow one to obtain from the value of $f_v(m)$ a reliable value of the black hole mass m_x or its low limit, as well as the optical star mass m_v. An independent estimate of the optical star mass m_v obtained from information about its spectral class and luminosity gives us test results. Additional test comes from information about the absence or presence of X-ray eclipses in the system. Effects of the non-zero dimension of the optical star, its pear-like shape, and X-ray heating on the absorption line profiles and the radial velocity curve are investigated. It is very significant that none of ten known massive $(m_x > 3M_\odot)$ X-ray sources considered as black hole candidates is an X-ray pulsar or an X-ray burster of the first kind.

A M Cherepashchuk P K Shternberg State Astronomical Institute, Universitetskiĭ prosp. 13, 119899 Moscow, Russia
Tel. (7-095) 939-28 58; Fax (7-095) 932-88 41
E-mail: cher@sai.msu.su

Received 4 April 1996
Uspekhi Fizicheskikh Nauk **166** (8) 809–832 (1996)
Translated by K A Postnov, edited by S D Danilov

1. Introduction

Black holes are predicted by Einstein's General Relativity (GR). The possibility of their observations is justified by Ya B Zel'dovich [1] and E E Salpeter [2], who predicted a powerful energy release during a nonspherical accretion of matter onto a black hole. It should be noted that as objects with the parabolic velocity equal to the speed of light black holes are formally (although not quite consecutively) predicted within the framework of the Newtonian gravitation, which was done by Mitchell and Laplace as early as in XVII century (see Refs [3, 4] for more detail). Binary stars as an instrument for black hole studies are proposed in Refs [5, 6] (see also Ref. [7]). The theory of accretion of matter from interstellar medium onto a single moving black hole is developed in Ref. [8] (see also Refs [9, 10]). The theory of disc accretion of matter onto black holes in close binary systems is elaborated in Ref. [11—14].

Theoretical predictions made in these references have been excellently confirmed by the results of subsequent X-ray observations obtained with specialised satellites, first and foremost with the american 'UHURU' satellite [15].

To date, tens thousand compact X-ray sources are discovered in our and nearby galaxies. Most of them are X-ray binary systems in which the optical star — donor supplies matter onto the neighbour relativistic object — a neutron star or a black hole. Accretion of this matter onto the relativistic object leads to a huge energy release in X-ray band with a luminosity of the order of 10^{36}–10^{39} erg s^{-1}, which is thousands and millions times higher than the bolometric luminosity of Sun.

The identification of first X-ray binary systems with optical stars revealed main reasons for optical variability: the reflection effect, more precisely, the heating of the optical star surface by the powerful X-ray emission from accreting relativistic object [16, 17], and ellipticity effect related to tidal

deformation of the optical star surface in the gravitational field of relativistic object [18, 19]. The reflection and ellipticity effects proved to be typical for X-ray binary systems. Observations of optical variability caused by these effects help in making a reliable optical identification of X-ray binary systems: the coincidence of periods and phases of optical and X-ray variability or the coincidence of X-ray and optical outbursts prove the identification reliability.

The optical star is a probe body in the gravitational field of a relativistic object. Photometrical and spectral observations taken by means of classical ground-based astronomy methods allow the optical star motion study and thus the relativistic object mass determination. Here, since the binary orbit size is by 5 – 7 orders of magnitude larger than the gravitational radius of the components, Newton's gravitational law is sufficient to determine component masses.

Those X-ray sources whose mass is measured to exceed 3 solar masses (an absolute upper limit on the neutron star mass predicted by the GR — see, for example, Ref. [20]) may be considered as candidates to black holes. Bounds on the X-ray source radius ($r < 1000$ km) follow from both the huge X-ray luminosity and rapid irregular variability of the X-ray flux on millisecond timescale.

The number of such high-mass compact X-ray sources — black-hole candidates known to date — amounts to ten and, owing to X-ray and optical astronomy successes, increases continuously. A notable fact is being gradually revealed: the black hole candidates differ form neutron stars not only in having higher masses, but also by observational appearances. In particular, none of ten reliable black hole candidates is either an X-ray pulsar, or a Type I X-ray burster, i.e. has signatures characteristic of accreting neutron stars.

The mass is the most important parameter needed to identify a relativistic object with a black hole. In the present review we describe astronomical aspects of black hole problem and first of all the methods and results of mass determination of relativistic objects in X-ray binary systems (see also reviews [21 – 24], which depict various aspects of black hole discovery, and also Refs [3, 4, 25], where black hole physics is described).

2. Main characteristics of X-ray binary systems

In most cases the optical star in an X-ray binary system is close to fill its critical Roche lobe [26], which determines a limiting equilibrium figure in the rotating reference frame connected with the binary system (see Fig. 1).

In the reference frame connected with the binary system's barycentre the equation for equipotential surfaces in the case of two point masses in circular orbits is written in the form

$$U = -\frac{Gm_1}{r_1} - \frac{Gm_2}{r_2} + \frac{1}{2}\,\omega^2(x^2 + y^2)\,, \qquad (1)$$

where U is the potential, m_1, m_2 are the masses of the components, r_1, r_2 are the distances from a given point to the first and second mass, respectively, ω is the orbital angular velocity, $x^2 + y^2$ is the square distance from the given point to the rotational axis of the system passing through its centre of mass, G is the Newtonian gravitational constant.

The critical Roche lobes (simply Roche lobes below) for the first and second components touch each other at the inner Lagrangian point. If a star is close to fill its Roche lobe, a matter outflow occurs from the vicinity of the Lagrangian point, predominantly in the form of a gas stream, onto the relativistic object, which leads to the formation of an accretion disc around it with a size comparable to its Roche lobe.

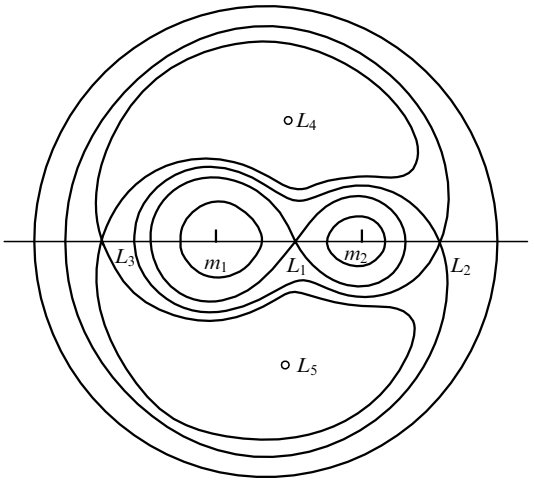

Figure 1. The family of equipotential surfaces in a close binary system approximated by the Roche model (the orbital plane cross-section). The mass ratio of the components is 0.5. Points $L_1 - L_5$ are the libration Lagrange points.

The theory of disc accretion of matter onto relativistic objects is developed in Refs [11 – 14]. Two- and three-dimensional gasdynamic calculations of gas flows in close binary systems with compact objects have been performed in the last years (see, for example, Refs [27 – 31]). The regime of disc matter accretion, in addition to the gravitational field of relativistic object and matter viscosity (which is usually connected with turbulence), is affected by some other factors: the rotation of the neutron star magnetosphere, radiation pressure (see, for example, Refs [12, 13, 32, 33]). In those cases when the influence of the gravitational field and viscosity is predominant, the accretion results in emerging a powerful X-ray source in the innermost parts of the accretion disc with a luminosity [24]:

$$L_{\rm x} = 0.057\dot{M}c^2 \approx (3 \times 10^{36}\,{\rm erg\,s^{-1}})\left(\frac{\dot{\rm M}}{10^{-9}{\rm M}_\odot\,{\rm year}^{-1}}\right)$$

for a non-rotating black hole and

$$L_x = 0.42\dot{M}c^2 \approx (3 \times 10^{37}\,{\rm erg\,s^{-1}})\left(\frac{\dot{\rm M}}{10^{-9}{\rm M}_\odot\,{\rm year}^{-1}}\right)$$

for a limit-rotating black hole, where $\dot{M}$ is the accretion rate from the disc to the black hole. For typical values $\dot{M} = (10^{-7} - 10^{-9})\,M_\odot$ the X-ray accretion luminosity attains $10^{36} - 10^{39}$ erg s^{-1}.

In the case of the optical star underfilling its Roche lobe accretion of matter onto the relativistic object proceeds mainly from the optical component's stellar wind [32, 34]. In that case the accretion disc size is small compared to the relativistic object's Roche lobe [34]. The characteristic radius of gravitational capture of stellar wind matter by the relativistic object (the Bondi–Hoyle radius [35]) is

$$r_{\rm B} \approx \frac{2GM_{\rm x}}{v_{\rm w}^2 + v_{\rm orb}^2} \approx 4R_\odot$$

for the supersonic stellar wind velocity $v_w = 1000$ km s^{-1} and the relativistic object's orbital velocity $v_{orb} = 100$ km s^{-1}. Here $M_x \approx 10 M_\odot$ is the mass of the relativistic object.

When the optical star fully fills its Roche lobe and in the case its mass is high (more than 10 solar masses), the thermal relaxation time-scale of the star is

$$t_K \approx 3 \times 10^7 \left(\frac{M}{M_\odot}\right)^{-2} < 3 \times 10^5 \text{ year},$$

and the rate of the matter supply into the disc becomes very high: $\dot{M} > 10^{-6} M_\odot$ /yr. In this case the accretion disc becomes optically thick for X-ray radiation from its central parts [36, 37]. An optically bright disc is then observed instead of an X-ray source. In this way a supercritical regime of disc accretion is realised, first described in Ref. [12]. In that case the accretion luminosity is restricted by the Eddington limit

$$L_E = (1.3 \times 10^{38} \text{ erg s}^{-1})\, \mu \frac{M_x}{M_\odot},$$

at which the radiation pressure force is comparable with the gravitation attraction force. Here μ is the molecular weight per one electron. Under the action of the radiation pressure, a powerful quasispherical outflow of matter with velocities about thousands km/s occurs from the central parts of the disc, and the 'disc' is a geometrically thick formation due to the presence of an opaque, extended, expanding atmosphere. A new and unexpected feature of the supercritical accretion onto relativistic object is the formation of strongly collimated (with the opening angle less than one degree) relativistic (velocity $\sim 0.26\,c$) jets of matter which are observed in the peculiar binary system SS433 [38, 39].

Ordinary sub-critical accretion discs are geometrically thin. However, since the disc thickness increases slowly with the distance from its centre, the outer parts of the disc intercept a small (a few percents) fraction of the flux from central parts, are heated and radiate in optical range [12] with a luminosity of a few percents of the compact object X-ray luminosity.

Main types of X-ray binaries are presented in Table 1 (see catalogues [40, 41] for more detail). It is seen that black holes happen in persistent X-ray binary systems with high-mass O–B stars, as well as in transient X-ray binaries with low-mass F–M stars (X-ray Novae).

3. On the criterion of the presence of a black hole in a binary system

The main features of an accreting black hole are: a high mass (more than three solar masses) and a powerful X-ray emission (luminosity of the order of $10^{36}-10^{39}$ erg s^{-1}) in the absence of X-ray pulsar or Type I X-ray burster phenomena. Note that among accreting neutron stars, too, there are objects showing no X-ray pulsar or X-ray burster phenomenon.

The X-ray pulsar phenomenon [42] is connected with canalising the accretion disc plasma by a strong magnetic field (of the order of 10^{12} G) of a rapidly rotating neutron star that has a solid surface. The matter penetrating through the magnetic poles forms high-temperature ($T \sim 10^7-10^8$ K) accretion columns there [43 – 45]. In addition, in a strong magnetic field the X-ray emission from the accretion columns becomes strongly beamed due to a high anisotropy of electron motion [46, 47]. All that, provided that the neutron star rotation axis does not coincide with the magnetic dipole axis, leads to the lighthouse effect and an X-ray pulsar phenomenon — a strictly periodic (with periods from fractions of second to thousands seconds) variability of the X-ray emission from the accreting neutron star.

The accretion of matter onto a neutron star with comparatively weak magnetic field (less than 10^{10} G) results in no X-ray pulsar phenomenon. However in this case for not too high accretion rates (less than 10^{-8} $M_\odot$/yr) thermonuclear explosions may occur on the neutron star surface caused by a thermonuclear burning instability in the degenerate matter of the accreting neutron star [48 – 50]. This leads to a Type I X-ray burster phenomenon, when irregularly repeating, short (the duration is of the order of 1 – 10 s), powerful (the luminosity at maximum is $\sim 10^{37}-10^{38}$ erg s^{-1}) X-ray bursts are observed against a persistent X-ray background [48].

During accretion of matter onto a stellar-mass black hole, no X-ray pulsar or Type I X-ray burster phenomena are expected to occur, since, according to the GR, a black hole has neither solid surface, nor strong magnetic field. For an accreting black hole one may expect only irregular variability

Table 1. Types of X-ray binary systems with relativistic objects.

Type	Optical star	Roche lobe filling	Relativistic object	Orbital period (days)	e	L_x, erg s^{-1}	Note
Persistent with O–B companions	O – È V–I, $m_v = (20-40)M_\odot$	almost	neutron star, black hole	1.4 – 10	0 – 0.1	$10^{36}-10^{39}$	stable
Transient with Be-stars	Be V–III $m_v = (10-30)M_\odot$	no	neutron star	8 – 600	0.2 – 0.8	$\leqslant 10^{37}-10^{38}$	transient $\sim$ 30 days
Persistent with F–M stars	F–M V–III $m_v = (0.1-1.5)M_\odot$	yes	neutron star	0.1 – 10	0	$\sim 10^{36}-10^{38}$	stable
Transient with F–M stars (X-ray Novae)	F–M IV–V $m_v = (0.1-2.3)M_\odot$	yes	neutron star, black hole	0.1 – 6.5	0	$\leqslant 10^{37}-10^{38}$	transient $\sim$ 30–120 days
X-ray bursters	$\sim$ M $m_v < 1M_\odot$	yes	neutron star	<1	0	$\leqslant 10^{37}-10^{38}$	bursts 1 – 10 s

Note: m_v is the optical star mass, e is the orbit eccentricity, L_x is the X-ray luminosity; the last column lists durations of X-ray outbursts.

of X-ray flux on timescales as short as $\sim r_g/c$, where $r_g = 2GM_x/c^2$ is the black hole's gravitational radius. Recently, quasi-periodic oscillations of X-ray flux were reported from accreting black holes, with frequencies from several hundredths to several tenths Hz, depending on the X-ray luminosity [51, 52]. The quasi-periodic oscillations of X-ray flux were discovered earlier for accreting neutron stars, but with higher frequencies – from several Hz to tens Hz [53]. For more detail on black hole criteria see, for example, Ref. [54].

It recently became clear that X-ray spectra of accreting neutron stars and black holes in binary systems are strongly different [55]. Spectral and temporal properties of accreting black holes are analyzed in detail in Ref. [56]. X-ray and gamma-observations performed over last years by orbital observatories Ginga, MIR-Kvant, Rosat, Granat, GRO and Asca have provided us with principally new information on spectral characteristics of accreting neutron stars and black holes (see, for example, Ref. [55 – 63]). In particular, it is found that accreting black holes show systematically harder X-ray spectra than neutron stars [59]. In spectra of some accreting black holes a narrow variable emission line at energies about ~ 500 keV is discovered, whose nature is not clear as yet and is under discussion [55, 59, 61, 62]. Three galactic X-ray binaries — black hole candidates (1E1740.7 – 2942, GRS1915 – 105, GRO1655 – 40) — revealed the presence of relativistic collimated jets with plasma velocities of $\sim$ 0.9c [64 – 66].

This allows us to elaborate some important indirect empirical criteria that may be used to identify compact X-ray sources with black holes, including the cases when their mass is unknown (see, for example, Refs [55, 56, 67, 68]).

In this review, we restrict ourselves to considering only those black hole candidates for which reliable mass estimates are available.

4. Optical appearances of X-ray binary systems

4.1 Ellipticity effect

The ellipticity effect of the optical star was discovered for the first time in X-ray binary system Cyg X-1 [18]. In the same paper [18] a method to estimate the orbital inclination angle by the ellipticity effect observed was proposed, which is effectively used in the last years to determine black hole masses in transient X-ray binaries (X-ray Novae) in quiescent state.

The form of a tidally distorted star in a close binary system can be described within the framework of a generalised Roche model which implies that the mass of the star is mainly contained close to its centre. This assumption is validated by observations of apsidal motion in several ten classical close binaries with elliptical orbits (see, for example, Ref. [69, 70]), according to which the empirically determined ratio of the matter density at the stellar centre to its mean density falls within the range of 50 – 600. This allows one to consider, to a good approximation, that the form of equipotential surfaces of the close binary system is practically independent of the degree of deformation of the optical star envelope, since its contribution to the total gravitational potential of the star is small compared to the contribution from central parts.

Generalising equation for the system potential (1) to elliptical orbits, let us write down the equation for the binary system potential in the rotating spherical reference frame with the origin at the binary system mass centre (see, for example, Ref. [71]):

$$U = \frac{1}{r} + \frac{q}{\sqrt{D^2 + r^2 - 2Dr\lambda}} - \frac{qr\lambda}{D^2} + \frac{1+q}{2} r^2 f^2 (1 - v^2) . \tag{2}$$

Here D is the instantaneous separation between the components at time t expressed in units of the large semi-axis of the relative orbit a:

$$D(t) = 1 - e\cos E(t) , \quad M(t) = E(t) - e\sin E(t) ,$$

E and M are the eccentric and mean anomalies, respectively, e is the orbit eccentricity [72], r is the modulus of radius-vector of a current point, λ, v are the corresponding direction cosines, $q = m_x/m_v$ is the mass ratio (with m_x, m_v being the mass of relativistic object and optical star, respectively), $f = \omega_{rot}/\omega_{orb}$ is the asynchronicity parameter of the optical star axial rotation and orbital revolution.

For elliptical orbits, the force field in the rotating reference frame connected with the components of such a system is time-dependent. However, if the orbital eccentricity is small ($e < 0.2$) and the optical star manages to come into a hydrostatic equilibrium state during a time interval much less than the time of the force changing, one may introduce an effective potential (2) at any point on the orbit. In that case one may consider (see, for example, Ref. [71]) a set of equipotential surfaces to exist at each moment of time, as in the case of the restricted three–body problem [72], which are analogous to Roche lobes for a circular orbit with synchronously rotating components.

The equipotential surface describing the optical star form is usually characterised by the optical star critical lobe filling factor μ which is the ratio of polar radii of partially and fully filled lobes:

$$\mu = \frac{R_z}{R_{z,cr}} , \qquad \mu \leqslant 1 .$$

Setting the parameter μ uniquely determines the potential U in Eqn (2) and the form of the optical star whose surface is a surface of equal potential. The factor μ of the critical lobe filling by the star is maximal at the orbit periastron and minimal at the apastron. A quasispherical form of the star corresponds to small $\mu < 0.5$, while for μ close to unity the form of the star becomes ellipsoidal and even pear-like.

In order to calculate the brightness of such a tidally-distorted star, one needs to take into account that the local effective temperature on the stellar surface depends on the modulus of the local gravity acceleration $g = |\mathrm{grad}\, U|$, and the field of radiation emanating from the stellar photosphere is anisotropic: the radiation intensity is maximal along the normal to the stellar surface and decreases with deviation from the normal (the limb darkening takes place).

The first effect, which is called gravitational darkening, is described by the formula

$$T_0 = \bar{T}_0 \left(\frac{g}{g_0}\right)^{\beta} , \tag{3}$$

where $\beta = 0.25$ for a radiative-equilibrium stellar envelope [73] and $\beta = 0.08$ for a convective stellar envelope [74]. Here $\bar{T}_0$ and g_0 are the mean effective temperature and the mean gravity acceleration on the stellar surface.

The second effect (the limb darkening) is calculated in radiation transfer theory for thin stellar atmospheres (see, for example, Ref. [75]) and to the first approximation is described by a linear (in $\cos\gamma$) limb darkening law

$$I = I_0(1 - x + x\cos\gamma)\,, \tag{4}$$

where γ is the angle between the line of sight and the normal to the stellar surface, x is the limb darkening coefficient ($0 \leqslant x \leqslant 1$).

The radiation intensity emitted by an elementary area $\mathrm{d}S$ on the stellar surface at a given wavelength λ in the direction with the angle γ to the normal is expressed in the form

$$\mathrm{d}I_\lambda = B_\lambda(T_0)\left[1 - x(\lambda,\, T_0)(1 - \cos\gamma)\right]\cos\gamma\,\mathrm{d}S\,, \tag{5}$$

where $B_\lambda(T_0)$ is the Planck function or the radiation intensity calculated using a stellar atmosphere model. Equation (5) together with expression (3) yield the emission law from each elementary area over the optical star surface. The total emission observed is obtained by summing up the fluxes from all visible areas (for which $\gamma < 90°$) in the observer's direction:

$$l(t) = \int\!\!\int \mathrm{d}I_\lambda\,. \tag{6}$$

The direction toward the observer is determined by the unit vector $\mathbf{a}$ along the line of sight, with components being easily calculated in the rotating frame [76]:

$$\mathbf{a} = (-\sin i\cos\theta,\ -\sin i\sin\theta,\ \cos i)\,, \tag{7}$$

where i is the orbital inclination (the angle between the line of sight and the orbital plane normal), θ is the angle of relative turn of the components ($\theta = 0$ when the optical star is at the front).

The coordinates of unit vector normal to an elementary area in the rotating reference frame are obtained in the form

$$\mathbf{n}_1 = -\frac{\mathrm{grad}\,U}{|\mathrm{grad}\,U|}\,. \tag{8}$$

The angle between the vectors $\mathbf{a}$ and $\mathbf{n}_1$ is determined from the scalar product

$$\cos\gamma = \mathbf{a}\cdot\mathbf{n}_1\,.$$

Using expressions (3) – (8) one may compute theoretical light curve $l(t)$ produced by the ellipticity effect as a function of the wavelength λ and parameters q, μ, i:

$$l(t) = l(t,\, \lambda,\, q,\, \mu,\, i)\,.$$

The light curve due to the ellipticity effect of the optical star has a double-wave shape (see Fig. 2, 3). The amplitude of the 'ellipsoidal' light curve increases when passing from hot stars of early spectral classes O–B to cool stars of late spectral classes K–M, which is connected with the limb darkening coefficient increase with decreasing the effective temperature of star. In Rayleigh-Jeans spectral region where $T_0 \propto I$ the surface brightness I changes comparatively weakly over the stellar surface $I \propto g^\beta$, where $\beta = 0.25$ or 0.08. So the ellipticity effect amplitude in this case is predominantly determined by a

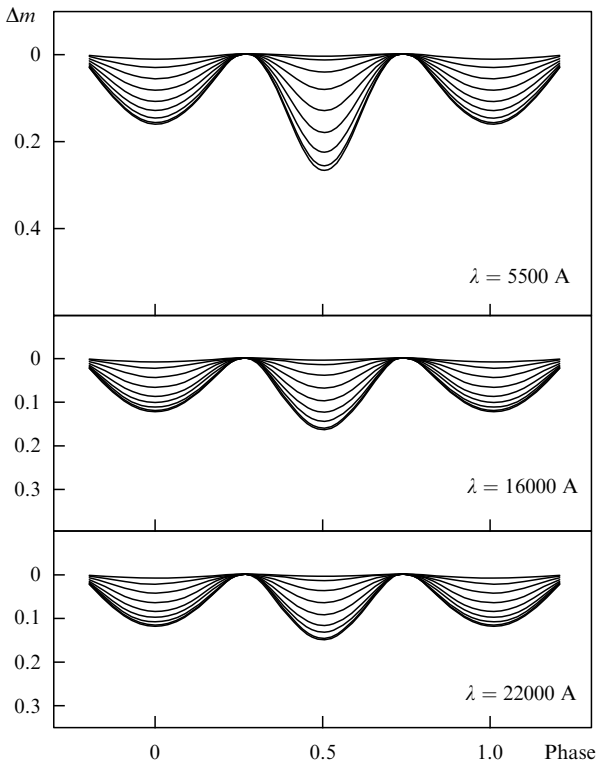

Figure 2. Theoretical optical and infrared light curves of an X-ray binary system caused by the optical star ellipticity effect for different orbital inclinations $i = 10°, 20°, 30°, 40°, 50°, 60°, 70°, 80°$ and 90°. Other parameters are: $q = m_x/m_v = 0.5$, $\mu = 1$, $\bar{T}_0 = 5000$K, $\beta = 0.08$, $k_x = L_x/L_v = 0$, $\kappa = 0$ ($\kappa = 0$ is the coefficient of X-ray radiation transformation in the optical star).

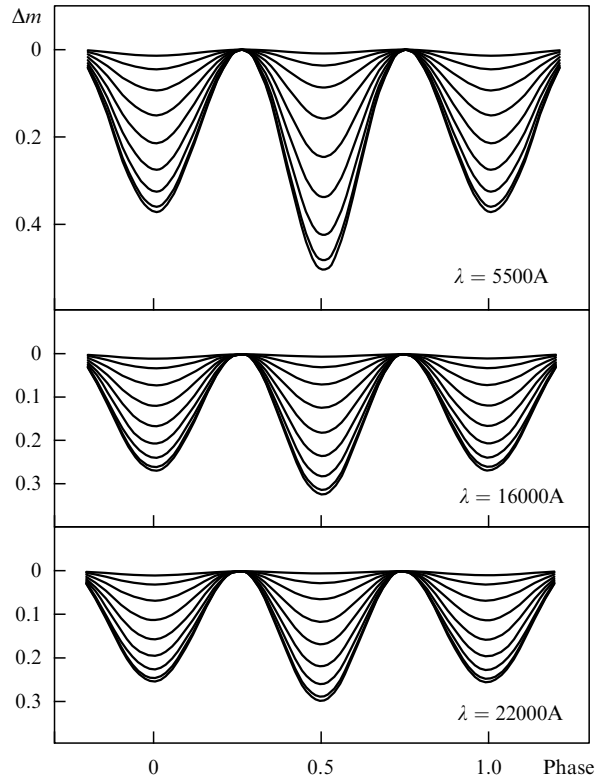

Figure 3. The same as in Fig. 2 for $q = 20$.

geometrical factor — the amount of tidal deformation of the star — and does not exceed 0.5 stellar magnitude ($0^m.5$, which is close to 50%).In the region, where the intensity depends exponentially on temperature, the surface brightness strongly varies over the stellar surface. In this case the geometrical form of the star plays the secondary role and the ellipticity effect amplitude tends to infinity. Due to the limb darkening effect, the 'ellipsoidal' light curve may have different minimum depths. For i close to 90° the light curve minimum corresponding to the case of the relativistic object being ahead is more pronounced, since, due to a pear-like shape of the star, the emission at these orbital phases comes to the observer at higher angles, on average, with respect to the normal to the stellar surface.

For elliptical orbits, the 'ellipsoidal' light curve may have maxima of different height (see Fig. 4), which is related to different tidal deformation of the star at different points on orbit. It is interesting to note that even in the case when $i = 0$ (the system orbit is perpendicular to the line of sight) the ellipticity of the orbit leads to brightness variations with an amplitude of a few hundredths stellar magnitude, since given an approximately constant volume of the star, the stronger tidal deformation, the larger the stellar surface is.

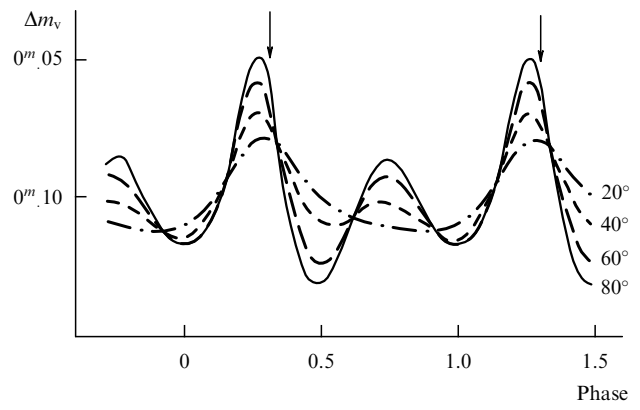

Figure 4. The dependence of the 'ellipsoidal' theoretical light curve form of an X-ray binary system with elliptical orbit at $e \approx 0.12$ and $\omega = 31°$ on the orbit inclination i marked by figures near the curves. The arrow shows the moment of the orbital periastron passage by the optical star. The inequality of maxima on the light curve is due to tidal deformation of the star at different points of the elliptical orbit.

When the asynchronicity parameter f deviates significantly from unity, the stellar form is mainly determined by centrifugal forces caused by rotation. The star becomes looking like an oblate spheroid, and under other equal conditions the ellipticity effect decreases. This happens in transient X-ray binary systems with hot Be-stars, in which optical stars are rapidly rotating and fill a small part of the Roche lobe.

The tidal and rotational deformations of the optical star lead to symmetry breaking and the appearance of a notable polarisation of optical radiation from X-ray binary systems (up to 0.5%), which is variable and correlates with the orbital period phase (see, for example, Refs [77 – 79]).

In transient X-ray binary systems with optical stars of late spectral classes F–M (X-ray Novae) the light curve due to the ellipticity effect demonstrates a long-term variability, which may be connected with the appearance, motion, and disappearance of spots on the stellar surface [80]. Fig. 5 – 11 show theoretical and observed light curves and radial velocity curves of X-ray binary systems, as well as a computer model for an X-ray binary system.

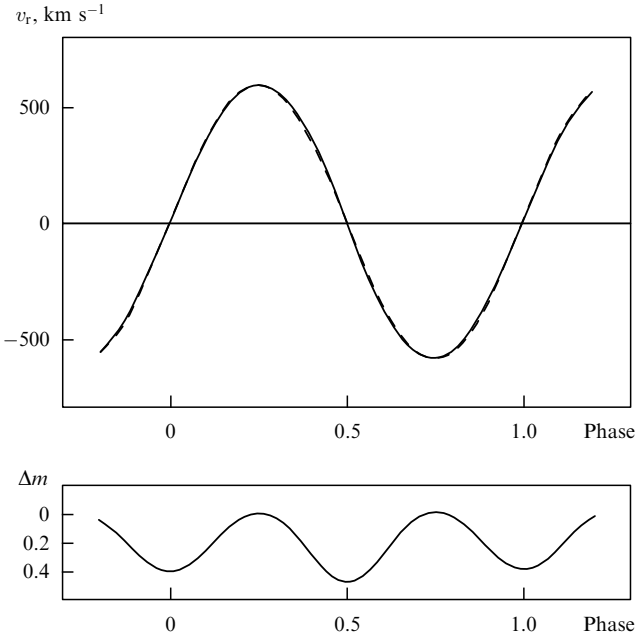

Figure 5. The theoretical light curve (at the bottom) and the radial velocity curve (at the top) for H_γ line calculated for an X-ray binary system with the parameters $q = 14.857$, $m_v = 0.7M_\odot$, $m_x = 10.4M_\odot$, $\mu = 1$, $i = 90°$, $P = 0^d,423$, $e = 0$, $\bar{T}_0 = 9000$ K, $k_x = 1$, $\kappa = 0.5$. The dashed radial velocity curve corresponds to the point-like optical star model, the solid line is the radial velocity curve for a pear-like tidally distorted star heated by the X-ray emission. The transition of the radial velocity curve through the γ-velocity (in the given case the γ-velocity is zero) corresponds to the brightness minima.

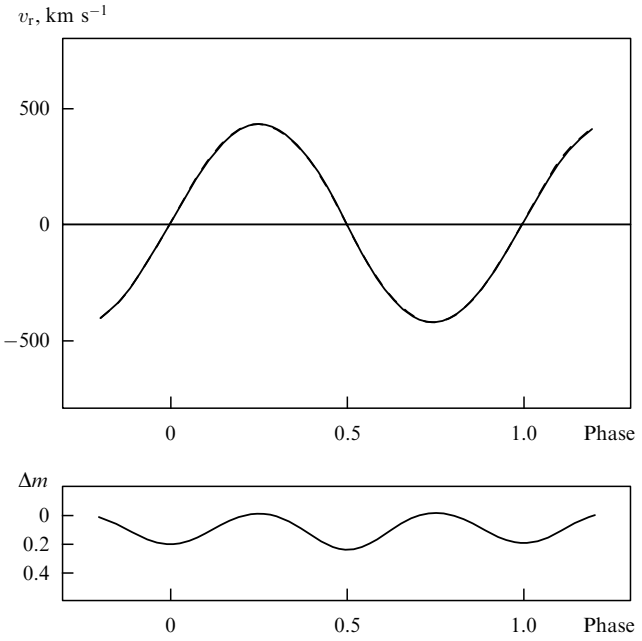

Figure 6. The same as in Fig. 5 for $i = 45°$.

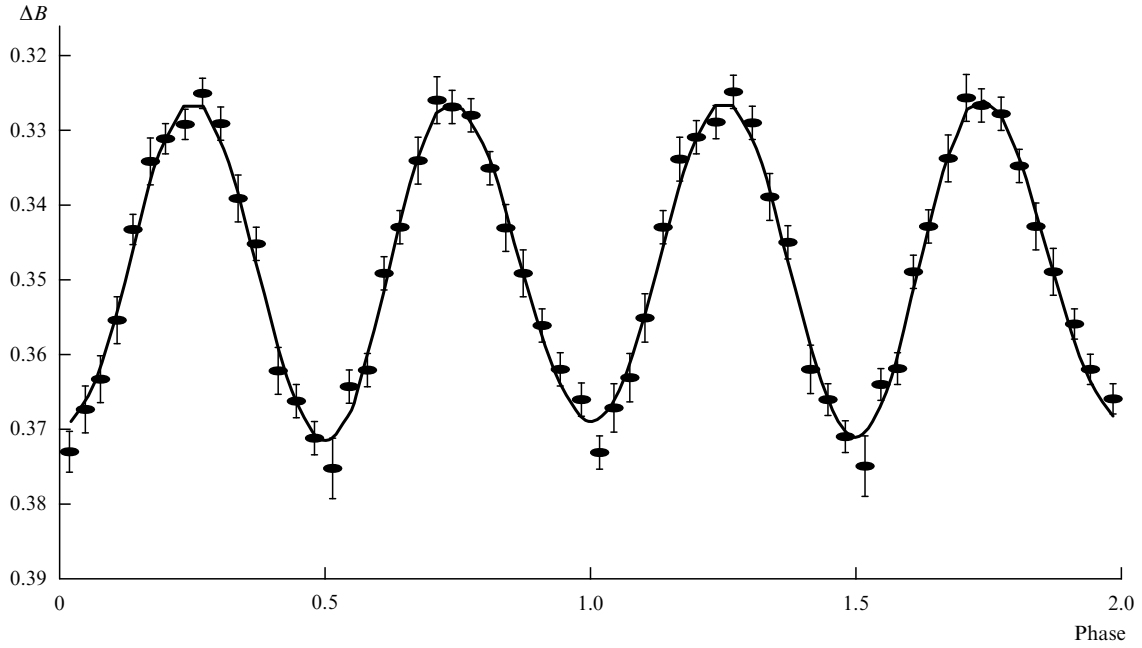

Figure 7. The optical light curve observed from X-ray binary system Cyg X-1. Here ΔB is the difference of stellar B-magnitudes ($\lambda = 4500$ A) . The solid line is the theoretical light curve calculated for the parameters $q = 0.45$, $i = 38^\circ$, $\mu = 0,90$.

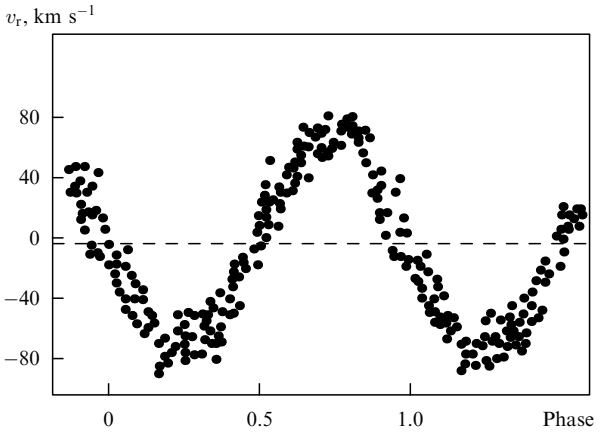

Figure 8. The radial velocity curve observed from Cyg X-1. Here v_r is the heliocentric radial velocity. The solid line marks the γ-velocity, the radial velocity of the system's barycentre.

In Fig. 7, 10 we present optical light curves of X-ray binary systems Cyg X-1 and XN Mus 1991 produced mainly by the ellipticity effect. The quantitative interpretation of these light curves permits one to determine the orbital inclination angle i, which is important for determination of relativistic object mass [81 – 84]. Very important is that the optical light curve enables us to justify the binary system model and the correctness of the relativistic object's mass determination: for almost circular orbits, if in the brightness minima the radial velocities of the components are equal to the radial velocity of the binary system's centre of mass, then the radial velocities measured reflect the orbital motion of the components and not their pulsations or motion of gaseous streams inside the system (see Figs 5, 6).

4.2 The effect of X-ray heating (the 'reflection effect')

For the first time the effect of X-ray heating of the optical component was discovered in HZ Her binary system [16, 17]. The heating of the optical star surface by the X-ray radiation from the compact object leads to increasing the temperature of the side of the star faced to the X-ray source, which leads to optical variability with the amplitude increasing with decreasing wavelength λ. The light curve due to the 'reflection effect' has a single-wave shape over the orbital period, whose amplitude in the case of X-ray binary systems may reach several stellar magnitudes. This is connected to the fact that the powerful X-ray source provides practically no light in optical range and the 'reflection effect' is observed here 'purely'. The fraction of the X-ray emission intercepted by the optical star is

$$\frac{r_v^2}{4a^2} \lesssim 6\,\%$$

(r_v is the stellar radius, a is the relative orbit radius), and if the X-ray luminosity L_x of the compact object appreciably exceeds the bolometric luminosity of the optical star, the 'reflection effect' amplitude may be fairly high, which takes place in the well-known X-ray binary system HZ Her (see Fig. 12).

The calculation of the reflection effect in classical close binary systems (see, for example, Ref. [75]) is a very difficult task, as in that case one should take into account non-zero size of the illuminating star and transfer of radiation from this star inside the companion's atmosphere. In the case of X-ray binary systems, there are two important simplifications of the problem: the X-ray source to a good approximation may be considered point-like, and besides, hard ($kT > 1$ keV) X-ray radiation practically does not disturb optical star's atmosphere, penetrate to a large optical depth, and is thermalised

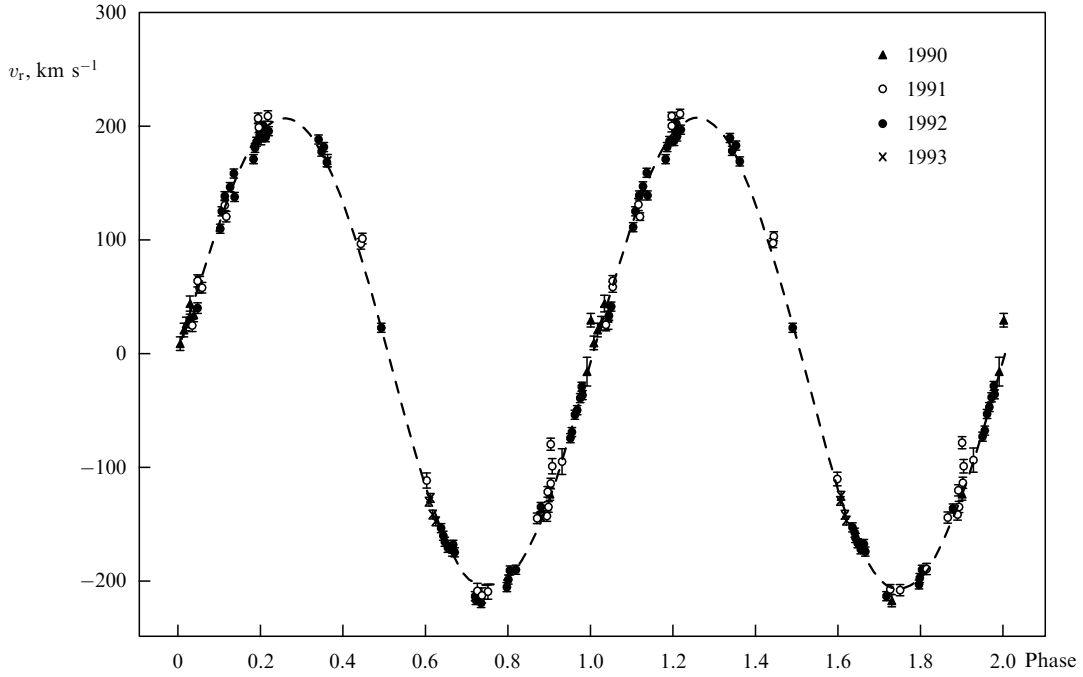

Figure 9. The radial velocity curve observed from X-ray binary system V404 Cyg (taken from Ref. [160]).

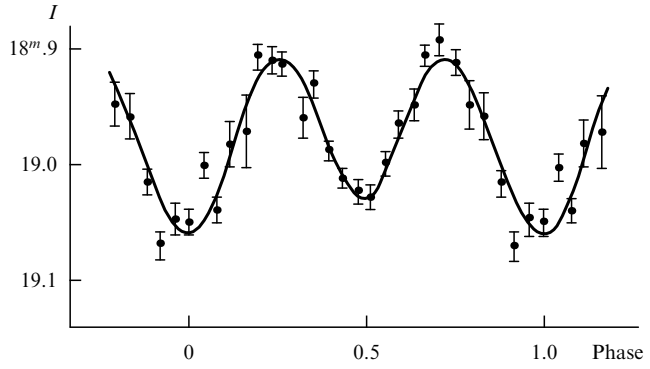

Figure 10. The observed (points) and theoretical light curves of X-ray Nova XN Mus 1991 in quiescence calculated for the parameters $q = 16$, $i = 40°$, $k_x = 6$, $m_x = 13M_\odot$.

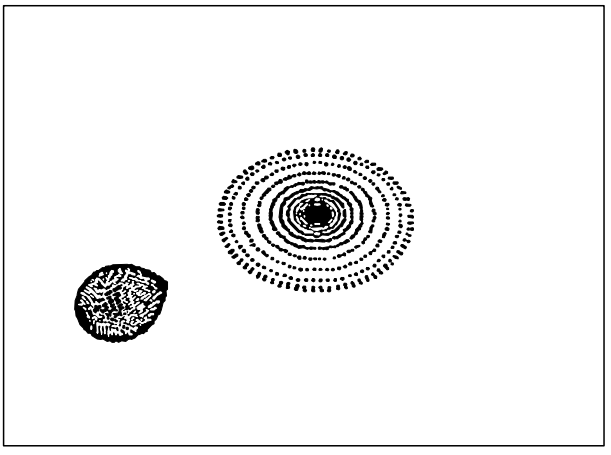

Figure 11. A computer model for XN Mus 1991 for $q = 16$, $i = 41°$, $m_x = 13M_\odot$.

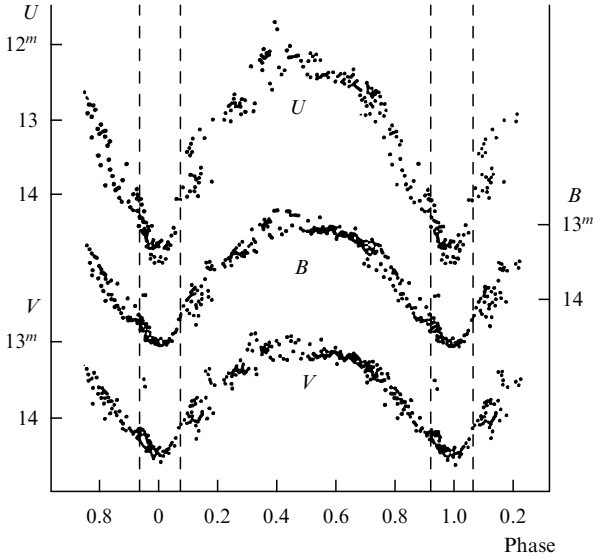

Figure 12. Optical *UBV* light curves of X-ray binary HZ Her produced mainly by the effect of the optical star heating by a powerful X-ray emission of the accreting neutron star. The vertical dashed lines isolate the X-ray eclipse region.

down there [85]. In this case, the resulting temperature of an elementary area on the surface of the illuminated optical star is determined by simply adding the density of proper outgoing radiation with that of the incident X-ray flux:

$$T = \left(T_0^4 + \frac{\kappa k_x L_v \cos\alpha \, F(\beta)}{4\pi\sigma\rho^2} \right)^{1/4}, \qquad (9)$$

where T_0 is the temperature of the area without heating calculated with account of the gravitational darkening (see

expression (3)), L_v is the bolometric luminosity of the optical star, ρ is the distance from the X-ray source to the centre of elementary area, $k_x = L_x/L_v$ is the ratio of bolometric luminosities of the optical star and X-ray source, κ is the coefficient of transformation of the X-ray emission inside the optical star, α is the angle between the normal to the area and the direction toward the X-ray source, β is the angle between the normal to the accretion disc plane and the direction toward the elementary area. The function $F(\beta)$ accounts for the X-ray emission anisotropy from the innermost parts of accretion disc around a black hole [12]:

$$F(\beta) = \frac{6}{7}\cos\beta(1 + 2\cos\beta)\,. \qquad (10)$$

For an accreting neutron star $F(\beta) = 1$.

Optical observations of the 'reflection effect' allow one to study characteristics of the X-ray source in a binary system even in those cases when the X-ray emission is not seen for a terrestrial observer. For example, in X-ray binary system HZ Her the X-ray source is visible only during 11 days from 35-day precession cycle and during remaining time it is in a turned-off state for a terrestrial observer. The fact that the amplitude and shape of the optical light curve of HZ Her then remains almost unchanged permits one to conclude that the X-ray source turning-off in this system is connected not with the cessation of accretion onto neutron star, but with geometrical screening of the X-ray source by a precessing accretion disc.

Transient X-ray binaries with low-mass F–M companions (X-ray Novae) exhibit the extremal case of the 'reflection effect'. In a quiescent state, when the system's X-ray luminosity is small (less than 10^{33} erg s^{-1}) the optical light curves of such systems demonstrate a typical ellipticity effect. During the X-ray outburst when $L_x = 10^{37} - 10^{38}$ erg s^{-1} the optical brightness of the system increases hundreds times, which is connected with heating of the optical star and especially of the accretion disc by a powerful X-ray emission from the compact object. It is important to note that since the components mass ratio in X-ray Novae is large, the optical star there takes a small solid angle and the X-ray emission is strongly screened by the accretion disc body, which leads to decreasing the optical star heating and dominating optical emission from the accretion disc. The optical outburst observations permit us to identify reliably the optical star with X-ray source.

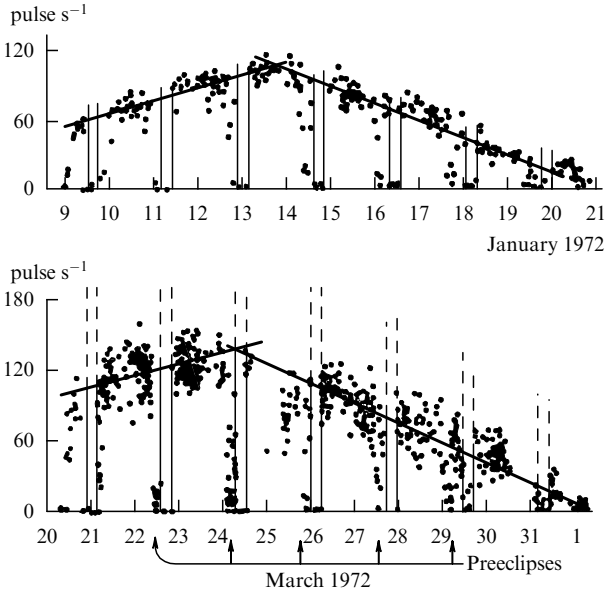

Figure 13. The 35-day modulation of X-ray emission of HZ Her = Her X-1. The narrow minima are X-ray eclipses with the orbital period of $1^d.7$. X-ray 'dips' are also seen, the preeclipses due to the X-ray source emission absorption by gaseous streams and dense clumps in outer parts of the accretion disc.

4.3 Eclipse and precession effects

Effects of optical eclipses of the accretion disc by the star and of the star by the disc, as well as effects relating to the disc precession, are most prominent in a peculiar X-ray binary system SS 433 containing a supercritical, optically-bright, precessing accretion disc [39, 86] (see Fig. 14). In classical X-ray binary systems, as already noted, the accretion disc optical luminosity is comparatively low, of the order of several percents of the X-ray luminosity of compact object. Some X-ray binaries with orbital inclination i differing not too much from 90° show X-ray eclipses caused by the optical star that have a characteristic Π-shaped form, since the X-ray source size is much less than the radius of the star (see Fig. 13). An analysis of the duration of X-ray eclipses allows one to impose some restrictions on the binary system parameters (see below). The effects of optical eclipse of accretion disc were first discovered in HZ Her system [19, 87, 88]. A model

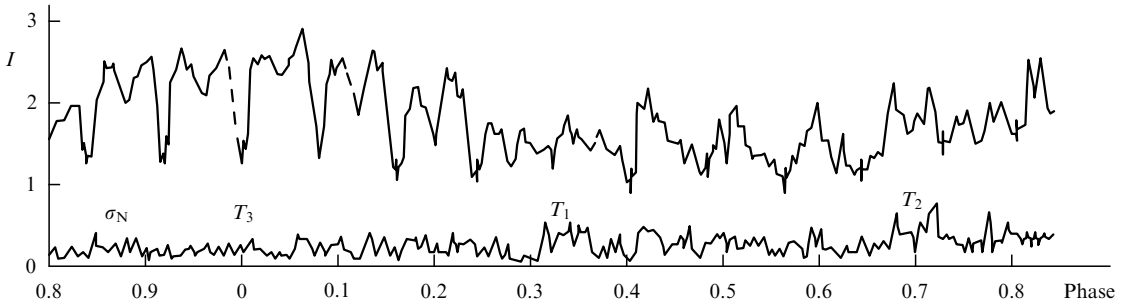

Figure 14. The optical light curve of X-ray binary SS433 within the precession period interval $162^d.5$. Optical eclipses of the accretion disc by the star and of the star by the disc once per orbital period $13^d.082$ are seen. The depth and shape of the eclipses, as well as the system's brightness out of eclipses, are modulated with the accretion disc precession period. At the bottom the mean-root-square amplitude σ_N of irregular brightness variations is shown which increases when the accretion disc is seen 'edge-on' (moments T_1 and T_2) and decreases at moments T_3 of the maximum accretion disc opening for a terrestrial observer.

explaining the long-term optical variability of HZ Her by precession of the accretion disc is considered in Refs [89, 90]. In X-ray Novae in quiescent state, when the X-ray luminosity is close to zero, accretion discs are observed around relativistic objects with an optical luminosity of about 10% of that of the star [91, 92]. A clear presence of a disc around relativistic object with almost zero X-ray luminosity ($L_x < 10^{33}$ erg s^{-1}) poses a difficult problem for accretion disc theory, especially in the case of X-ray Novae with black holes, in which it seems impossible to explain the absence of X-ray radiation by a magnetospheric propeller effect of a rapidly rotating neutron star.

Search for precession effects led to the discovery of a long-term variability in some X-ray binaries: HD 77581, $P_{\rm prec} = 93.3$ days [93], Cyg X-1, $P_{\rm prec} = 294$ days [94, 95], LMC X-3, $P_{\rm prec} = 198$ days [96].

The precession variability may be connected with an asymmetric supernova explosion in a binary system [97, 98]: the supernova explosion may turn the binary orbital plane relative to the normal star's rotation axis, which further leads to a forced precession of the star's rotation axis and the formation of a precessing or 'slaved' disc around the relativistic object [11, 89, 97]. In transient X-ray binaries with low-mass F–M components the X-ray outburst may be accompanied by the formation of an elliptical accretion disc around the relativistic object with a hot spot at the site of the collision of the gaseous stream from optical star with the disc outer boundary (see, for example, Refs [99, 100]). The major semiaxis of such a disc may slowly turn [101], which also causes the system's long-term variability in the case when the contribution of the optical emission from the disc and the hot spot into the total optical flux from the system is relatively large.

To account for optical eclipses and accretion disc precession, a reference frame related to the disc with the origin at the disc centre is introduced. In this reference frame an equation of the disc surface and a temperature distribution over it according to accretion disc theory are set (see, for example, Ref. [12]). Using transition equations one may write down the disc surface equation in the reference frame connected with the optical star mass centre [102]. The check that a given elementary area $\mathrm{d}S$ on the stellar surface is eclipsed by the accretion disc body is implemented as follows. A straight line passing through the area centre is drawn parallel to the line of sight (i.e. the vector $\mathbf{a}$, see expression (7)), and the condition of this line crossing with the accretion disc surface is checked. If no crossing occurs, the area $\mathrm{d}S$ is not eclipsed by the accretion disc body and its contribution should be taken into account when calculating the total brightness of the system (see expression (6)). The condition of the disc eclipse by the optical star is checked in a similar way.

Thus the quantitative account of the effects of ellipticity, 'reflection', and precession enables us to calculate (synthesise) the theoretical light curve of an X-ray binary system, the comparison of which with the observed light curve allows us to put some bounds on the plausible parameters of the system. For i close to 90°, optical light curves of X-ray binaries can be distorted by the absorption of the optical star light by gaseous streams and semitransparent stellar wind (see, for example, Refs [103 – 105]).

For more detail on methods of optical light curve synthesis in binary systems and statistical estimations of parameters and their confidence intervals (errors) see monograph [76].

5. Analysis of radial velocity curves

Optical spectral observations allow, by means of measuring Doppler line shift in the optical star spectrum caused by its orbital motion, the construction of the radial velocity curve of the optical star $v_r(t)$, i.e. the time dependence of the line-of-sight projection of the total velocity of star. If an X-ray pulsar is observed in the binary system, then by observing the Doppler shift in X-ray pulses arrival times one can construct the X-ray pulsar radial velocity curve. The radial velocity curve interpretation permits one to determine the masses of the components and the system's absolute size within an accuracy of its inclination i which is derived from additional data, for example from the light curve analysis.

As already noted, to determine masses of the components in an X-ray binary system it is sufficient to use Newton's gravity law. We do not deal here with the case of radiopulsars in binary systems, where a huge accuracy of pulsar motion determination allows us to observe relativistic effects and, usig them, to determine masses with a high accuracy and even to observe a secular decreasing of the orbital period due to gravitational wave radiation from the binary system [106, 107].

Let us consider a system of two point masses on an elliptical orbit (see, for example, Ref. [108]). The spectroscopic orbit elements of one of the system components are: the observed orbital period P connected to the true period P_0 by the relationship accounting for Doppler effect

$$P_0 = P\left(1+\frac{\gamma}{c}\right)^{-1}, \tag{11}$$

where γ is the radial velocity of the system's barycentre (since usually $\gamma \ll c$, P and P_0 differ insignificantly), the orbit eccentricity e, the periastron longitude ω that characterises the orbit orientation in the orbital plane relative to the observer, the semi-amplitude of the component's radial velocity K, the major semiaxis of the component's orbit a, the moment of the periastron passage T_1, the orbit inclination i characterising the orbit orientation in space (the value of i cannot be derived from the radial velocity curve).

Let us consider the orbit of one of the components with respect to the system's barycentre. We introduce a polar coordinate system (r, v) in the orbital plane, where r is the radius-vector of the star on the orbit, v is its polar angle (the true anomaly [72]). The line-of-sight projection z of the radius-vector is written in the form

$$z = r\sin i\sin(v+\omega)\,. \tag{12}$$

Differentiating relationship (12) with respect to time and using first and second Kepler's laws [72], it is easy to obtain the main equation connecting the observe radial velocity curve $v_r(t)$ with the orbital elements:

$$v_r(t) = \gamma + K\left[e\cos\omega + \cos(v+\omega)\right], \tag{13}$$

where

$$K = \frac{2\pi a\sin i}{P_0\sqrt{1-e^2}}\,. \tag{14}$$

The relation between the true anomaly v and time t is given by formulas for elliptical motion known from celestial

mechanics [72]:

$$M = \frac{2\pi}{P_0}(t - T_1), \tag{15}$$

$$M = E - e\sin E, \tag{16}$$

$$\tan\frac{v}{2} = \sqrt{\frac{1+e}{1-e}}\tan\frac{E}{2}, \tag{17}$$

where M, E, v are the mean, eccentric and true anomaly, respectively. From equation (13) it follows that the radial velocity of the star reaches its extrema at the orbit nodes when the star crosses the picture plane.

Solving the inverse parametric problem (13) – (17), one may determine the spectroscopic orbit elements of one of the components from $v_r(t)$, the radial velocity curve observed. If radial velocity curves are observed for both components of a binary system, one may find the orbital elements for each component, in particular, the quantities $a_x \sin i$ and $a_v \sin i$, where a_x and a_v are the major semiaxes of absolute orbits of the X-ray source and the optical star, respectively. Then, using the third Kepler's law

$$m_x + m_v = \frac{4\pi^2}{G}\frac{(a_x + a_v)^3}{P_0^2}$$

and the system's barycentre definition

$$\frac{m_x}{m_v} = \frac{a_v}{a_x},$$

one may find masses of the optical and X-ray component m_v and m_x to the factor $\sin^3 i$ accuracy.

Passing to units convenient for astronomical applications, let us write down the main formulae for the determination of masses and absolute sizes of the binary system

$$a_x \sin i = 1.375\times10^4(1-e^2)^{1/2}K_x P_0, \tag{18}$$

$$a_v \sin i = 1.375\times10^4(1-e^2)^{1/2}K_v P_0, \tag{19}$$

$$(a_x + a_v)\sin i = 1,375\times10^4(1-e^2)^{1/2}(K_x + K_v)P_0, \tag{20}$$

$$m_x \sin^3 i = 1.038\times10^{-7}(1-e^2)^{3/2}(K_x + K_v)^2 K_v P_0, \tag{21}$$

$$m_v \sin^3 i = 1.038\times10^{-7}(1-e^2)^{3/2}(K_x + K_v)^2 K_x P_0, \tag{22}$$

where m_x, m_v are expressed in Solar masses ($M_\odot$), a_x, a_v are in kilometres, P_0 is in days (P_0 is connected to P by expression (11)), K_x, K_v are in km s^{-1}.

If no X-ray pulsar is observed in X-ray binary system (in the case of a black hole), we have only one radial velocity curve for the optical star. In that case only so-called mass function of the optical star $f_v(m)$ is determined:

$$f_v(m) = \frac{m_x^3 \sin^3 i}{(m_x + m_v)^2} = 1.038\times10^{-7}(1-e^2)^{3/2}K_v^3 P_0. \tag{23}$$

The mass function of optical star bears information mainly on the mass of the unseen component (black hole) m_x that is expressed in the form

$$m_x = f_v(m)\left(1 + \frac{m_v}{m_x}\right)^2 \frac{1}{\sin^3 i}, \tag{24}$$

where quantities i and $1/q = m_v/m_x$ must be found from additional data, for example from the optical light curve analysis and the X-ray eclipse duration. Since $m_v/m_x > 0$ and $\sin i \leqslant 1$, from expression (24) it follows that the mass function of optical star $f_v(m)$ is an absolute lower limit to the X-ray source mass

$$m_x > f_v(m). \tag{25}$$

If an X-ray pulsar is observed in a binary system and its radial velocity curve is known while that for the optical star is unknown (for instance, because no reliable optical identification of the X-ray binary exists), one may find only the X-ray pulsar's mass function $f_x(m)$:

$$f_x(m) = \frac{m_v^3 \sin^3 i}{(m_x + m_v)^2} = 1.038\times10^{-7}(1-e^2)^{3/2}K_x^3 P_0. \tag{26}$$

The mass function of X-ray pulsar bears information on the optical star mass m_v that is expressed as

$$m_v = f_x(m)\left(1 + \frac{m_x}{m_v}\right)^2 \frac{1}{\sin^3 i}. \tag{27}$$

The mass function of X-ray pulsar $f_x(m)$ is an absolute lower limit to the optical star mass m_v:

$$m_v > f_x(m). \tag{28}$$

Expressions (21) – (28) enable us to estimate masses of the optical star and relativistic object within the framework of the two point masses model.

The assumption of the point-like masses is valid for a relativistic object, since the size of X-ray emitting region is $\sim 10^8$ cm [12], which is by 3 – 5 orders lower than the binary system size and by 2 – 4 orders lower than the optical star radius. For an optical star, the model of point-like object in many cases is incorrect. It is needed to check how a non-zero size of the optical star affects the mass determination.

Since optical stars in X-ray binaries in most cases are close to fill their Roche lobes, for the mass ratio $q < 1$ (Fig. 15) the binary system barycentre lies inside the optical star body. In

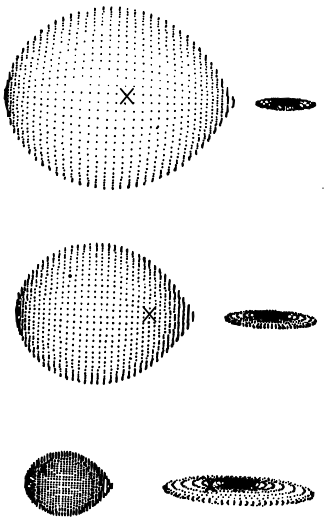

Figure 15. Computer models of an X-ray binary system for $q = 0.1$ (at the top), $q = 0.5$ and $q = 10$ (at the bottom). The orbit inclination is $i = 80$. The orbital period phase is $\varphi = 0.25$. The cross marks the position of the binary system's barycentre.

that case the parts of the optical star lying at different sides of the system's barycentre move in the opposite directions when the star is in orbital motion. This fact together with the action of the ellipticity and 'reflection' effects may lead to a strong distortion of the radial velocity curve of the optical star. The radial velocity curve synthesis of close binary systems with account of the ellipticity and 'reflection' effects were considered in Refs [109 – 115]. In particular, Ref. [113] considers the influence of X-ray heating effect on the measured radial velocities of absorption lines and shows that these effects can be significant even for X-ray binaries with a small ratio $k_x = L_x/L_v$, in which the X-ray heating affects weakly the light curves. Soft X-ray quanta with energies 1 keV, by being absorbed in the optical star atmosphere, cause the temperature distribution inversion in the upper atmospheric layers and, as a consequence, the appearance of an emission component of a line, which, by superposing with the absorption line, causes the line profile distortion and the distortion of the corresponding radial velocity curve of the optical star. Therefore, when analyzing the radial velocity curves of X-ray binaries it is necessary to take into detailed account the soft X-ray component contribution to the total X-ray flux from the system.

Calculations performed in Refs [113, 114] are useful for a qualitative analysis of the X-ray heating effect but require a lot of computer time. To solve the inverse problem of the spectroscopic orbit parameters determination, an efficient method for calculating theoretical line profiles from real stars is required that allows multiple radial velocity curve calculation. To date, large calculations of the absorption line profiles in stellar atmospheres have been performed for various values of the gravity acceleration g and effective temperature $T_{\rm eff}$ [116]. This provides us with the possibility to elaborate algorithms for synthesising radial velocity curves of tidally-deformed stars in binary systems with account of the heating effect, which are available for broad application to analyze the radial velocity curves observed. In Ref. [115], a method for theoretical spectral line profiles and radial velocity curves synthesis in close binary systems is developed that takes into account the tidally-rotational distortion of the components form, the gravitational darkening, the limb darkening, the heating by the radiation from the neighbour component, the motion of stellar wind plasma close to the star's photosphere.

The radial velocity curve synthesis for an X-ray binary system is similar to the light curve synthesis described above (see expressions (2) – (10)), with the only difference that now not only radiation intensity at a given wavelength λ is put into correspondence to each elementary area $\mathrm{d}S$ on the optical star surface, but a set of intensities for close λ (the local absorption line profile for given g and T) is ascribed to the area. In addition, Doppler shifts of all local profiles connected with the orbital revolution of the star, its axial rotation, the expansion of its stellar wind, are taken into account. The resulting radial velocity of the area $\mathrm{d}S$ is [115]:

$$v_r = v_0 + v_w + V_c + \gamma\,, \tag{29}$$

where $v_0 = -\mathbf{v}_0 \cdot \mathbf{a}$ is the line-of-sight projection of the velocity vector of the area (see expression (7)), $\mathbf{v}_0 = [\boldsymbol{\omega} \times \mathbf{r}]$, where $\boldsymbol{\omega}$ is the angular orbital velocity vector (the orbital and axial rotations are assumed to be synchronous), $\mathbf{r}$ is the radius-vector of the area $\mathrm{d}S$, v_w is the line-of-sight projection of the stellar wind velocity $\mathbf{v}_w$ close to the star's photosphere (which is assumed to be proportional to the local speed of sound and directed along the normal to the stellar surface — see expression (8)), V_c is the line-of-sight projection of the orbital velocity of the star's centre of mass relative to the system's barycentre, γ is the radial velocity of the system's barycentre.

For an area $\mathrm{d}S$ with temperature T and gravity acceleration $g = |\mathrm{grad}\, U|$ (see expression (2), (3), (9)), by applying the interpolation procedure and using line profile tables (see Ref. [116]), the local profile $H_{\rm loc}(\lambda)$ normalised to the local continuum is calculated. For an area $\mathrm{d}S$ with the local radial velocity v_r (see expression (29)), the profile $H_{\rm loc}(\lambda)$ should be shifted by $\Delta\lambda = \lambda_0 v_r/c$, where λ_0 is the central wavelength of the unshifted line. Using expression (5), the local continuum is calculated for the area $\mathrm{d}S$ (where T_0 should be substituted by T from expression (9)). Then, summing over all visible surface of the star (the angle $\gamma < 90°$) and taking into account eclipse effects, we calculate the total line profile from the star:

$$H(\lambda) = \int\!\!\int H_{\rm loc}(\lambda)\ \mathrm{d}I_\lambda\,. \tag{30}$$

The results of calculations of the optical star radial velocity curves for a realistic model for an X-ray binary system and their comparison with the radial velocity curves for two point mass model are shown in Figs 16, 17. It is seen that the difference is minimal for large mass ratios $q > 1$ (for which the optical star size is relatively small) and strongly increases for small $q < 1$ with increasing the X-ray heating effect characterised by the parameter $k_x = L_x/L_v$. In parti-

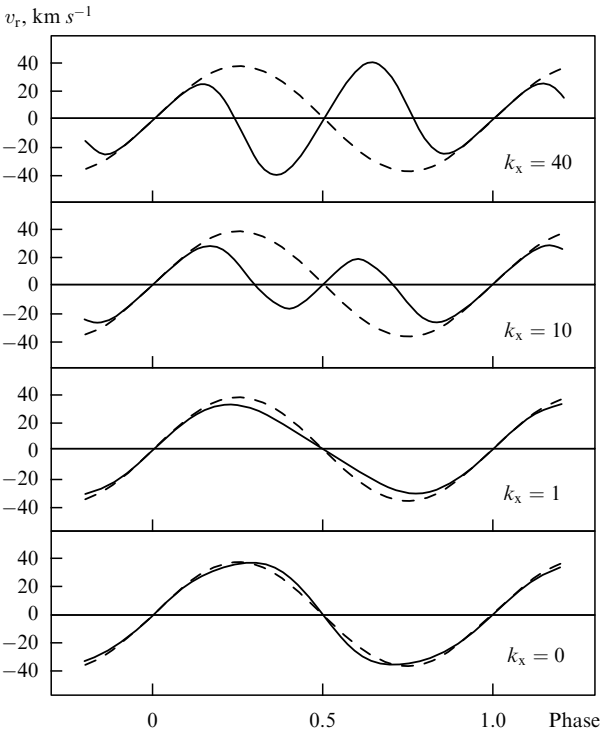

Figure 16. Theoretical radial velocity curves of an X-ray binary system calculated for a point-like optical star model (dashed lines) and a realistic stellar model with account of the ellipticity and X-ray heating effects. The parameters are: $q = 0.1$, $m_v = 10M_\odot$, $\mu = 0.9$, $i = 90°$, $T_0 = 9000$ K, $P = 1^d.5$, $e = 0$, $\kappa = 0.5$. The X-ray heating parameter k_x decreases from top to bottom. Differences are maximal for large k_x.

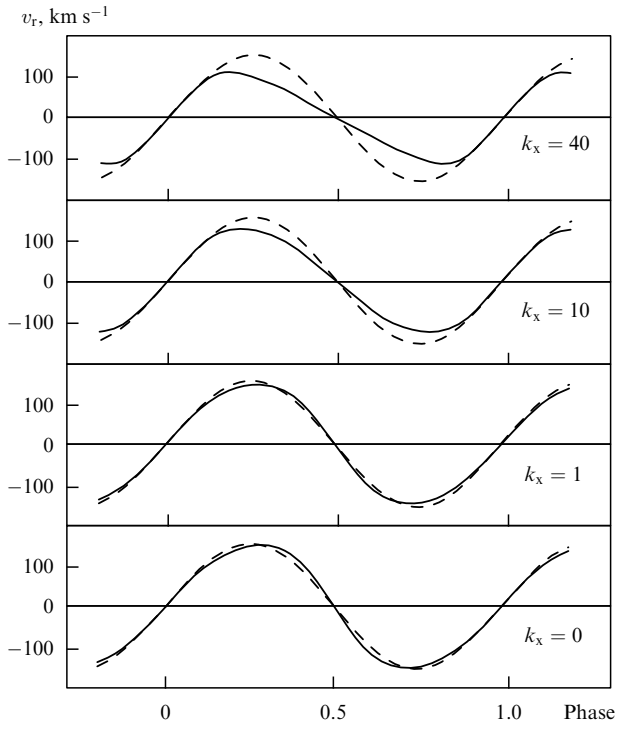

Figure 17. The same as in Fig. 15 for $q = 0.5$, $\mu = 2$.

cular, for $q = 0.1$, $k_x = 40$, $i = 70°$, and $\mu = 1$ the realistic radial velocity curve differs from the idealised one even in having different sign. This is due to the fact that the X-ray heated optical star part at $q = 0.1$ moves in the same direction as the X-ray source when in orbital revolution around the system's barycentre. This effect also holds when the Roche lobe filling degree of the optical star decreases from 1 to 0.7. The effect weakens for higher q.

Thus, our calculations show [115] that the point model for the optical star is well applicable to large $q > 5$, i.e. for most transient X-ray binaries with low-mass optical F–M stars (X-ray Novae), in which q attains 10 – 20. Therefore, to estimate black hole masses in X-ray Novae the two point mass model may be used to a good approximation (see expressions (18) – (27)). For small $q < 1$ (persistent X-ray binaries with O–B optical stars), when estimating components' masses it is needed to take into account a non-zero size of the optical star, its tidal deformation and the X-ray heating effect. The methods presented above enable us to make correct estimations of black hole masses within the framework of a realistic model for an O–B star.

One more distorting factor for the radial velocity curve of the optical star is connected with a selective star's light absorption in line frequencies in the anisotropic stellar wind and gaseous streams in the binary system (see, for example, Ref. [117]). This effect is minimal for X-ray Novae in quiescence when the stellar wind from optical F–M stars is negligibly small. It also decreases with decreasing i.

We do not consider specific observational problems connected with high-precision measurements of radial velocities in X-ray binaries, especially in X-ray Novae in quiescence when the binary system brightness is very weak ($V = 17$–22). A specific cross-correlation technics for constructing radial velocity curves of optical F–M star in X-ray Novae is described, for example, in Ref. [118].

The X-ray pulsar mass function $f_x(m)$ is determined most reliably, because the point-object model is well applied for a compact X-ray source and the plasma of the stellar wind and gaseous streams in binaries is transparent for X-ray photons with energies more than 1 keV.

6. Mass determination

6.1 The case of an X-ray pulsar

Methods for analysis of radial velocity curves and light curves of X-ray binary systems presented above are used to determine the mass of relativistic objects. Masses of X-ray pulsars in binaries with X-ray eclipses are determined most easily (see, for example, Ref. [119]). In this case, radial velocity curves of the X-ray pulsar and optical star allow us to determine $m_x \sin^3 i$ and $m_v \sin^3 i$ using expressions (21) and (22), as well as to find the mass ratio

$$q = \frac{m_x}{m_v} = \frac{K_v}{K_x} . \tag{31}$$

Therefore, to determine component masses m_x and m_v when an X-ray pulsar is present in the binary system, it is sufficient to evaluate only one parameter — the orbital inclination i. As already noted, the value of i can not be derived from an analysis of radial velocity curves of the system's components, and to evaluate it an additional information on the system is needed.

If an X-ray eclipse with the duration D is observed in a binary system containing X-ray pulsar, an independent relationship connecting parameters q, μ, and i with each other exists:

$$D = D(q, \mu, i) . \tag{32}$$

For example, in the case of a spherical star on circular orbit equation (32) takes the form:

$$D = \frac{1}{\pi} \arccos \frac{\sqrt{1 - r_v^2}}{\sin i} .$$

The X-ray eclipse durations D are calculated within the framework of the Roche model for a broad range of parameters q, μ, and i both for circular and elliptical orbits (see, for example, Ref. [120]).

If the optical light curve of an X-ray binary system demonstrates a significant ellipticity effect, one may assume that the Roche lobe filling degree of the optical star is close to unity: $\mu = 1$. Then the parameter i is found from equation (32) for known q and fixed $\mu = 1$, which allows us to determine the masses m_x and m_v. In this way first X-ray pulsar masses in eclipsing X-ray binaries were determined [119]. The assumption that $\mu = 1$ in this case is based only on qualitative considerations that amplitude of the system's optical variability caused by the ellipticity effect is large. In addition, only a small fraction of X-ray binary systems reveals eclipses of the X-ray source by optical star, since for this the orbit inclination i should be close to 90°.

For a more precise determination of μ, a qualitative interpretation of the optical light curve of the X-ray binary system $l(t)$ is required (which can be synthesised as described above):

$$l(t) = l(t, q, \mu, i, r_d, L_d) , \tag{33}$$

where r_d, L_d are, respectively, the radius and optical luminosity of the accretion disc within the framework of the simplest model of a circular accretion disc lying in the orbital plane. Since in most classical X-ray binaries optical eclipse effects are relatively small, theoretical estimates may be taken for r_d and L_d (see, for example, Refs [12, 121]): $L_d \sim 0.01\, L_x$, and r_d may be taken half the maximum Roche lobe radius of the relativistic object. In addition, the accretion disc optical luminosity L_d may be evaluated from spectrophotometric observations of the X-ray binary system by comparing equivalent widths of absorption lines from optical star in the binary system with the equivalent widths of a single star of the same spectral class and luminosity. Thus, the optical light curve $l(t)$ also allows us to constraint the permissible area of the parameters.

Paper [122] proposed to use information on the distance d to the binary system to restrict its parameters. If the distance to the system, d, and the interstellar absorption A_V are known, the visual stellar magnitude V of the optical star and its spectral class (which determines the effective temperature $T_{\rm eff}$) make it possible to determine the mean radius R_v of the optical star from the expression [123]:

$$A_V = V + 5.16 - 5\lg\frac{d}{R_v} - \frac{29000}{T_{\rm eff}}\,, \tag{34}$$

where d is in parsecs, R_v is in Solar radii. Then from the expression for the optical star mass function and third Kepler's law and using approximation formula for the mean Roche lobe radius R_{cr} one may obtain the relation between the parameters q, μ, and i:

$$\sin i = \frac{0.38\mu}{R_v}\sqrt[3]{\frac{GP_0^2 f_v(m)}{4\pi^2}}\,\frac{1+q}{q^{1.208}}\,, \tag{35}$$

where G is the Newton's gravity constant.

Finally, if spectroscopic observations of the optical star in an X-ray binary system are made with a very high spectral resolution and the broadening of absorption line profiles of the optical stars caused by its axial rotation is measured, then assuming synchronicity of the axial and orbital rotations and $\mu = 1$ (which is a reasonable assumption for X-ray Novae) one may derive q from the equation [124, 125]:

$$v_{\rm rot}\sin i = 0.462 K_v\,\frac{1}{q^{1/3}}\left(1+\frac{1}{q}\right)^{2/3}\,, \tag{36}$$

where the quantities $v_{\rm rot}\sin i$ and K_v are determined from spectral observations (Figs 18, 19).

Thus, Eqns (32), (33), (35), and (36) allows us to evaluate the parameters q, μ, and i. The parameter i permits the unique determination of the X-ray pulsar and optical star masses from the quantities $m_x \sin^3 i$ and $m_v \sin^3 i$.

6.2 The case of a black hole

Now we pass to the main question on the determination of black hole masses in X-ray binary systems. In this case an X-ray pulsar is absent and we have only the optical star mass function $f_v(m)$ from which the expression for black hole mass is derived (see Eqn (24)):

$$m_x = f_v(m)\left(1+\frac{1}{q}\right)^2\frac{1}{\sin^3 i}\,. \tag{37}$$

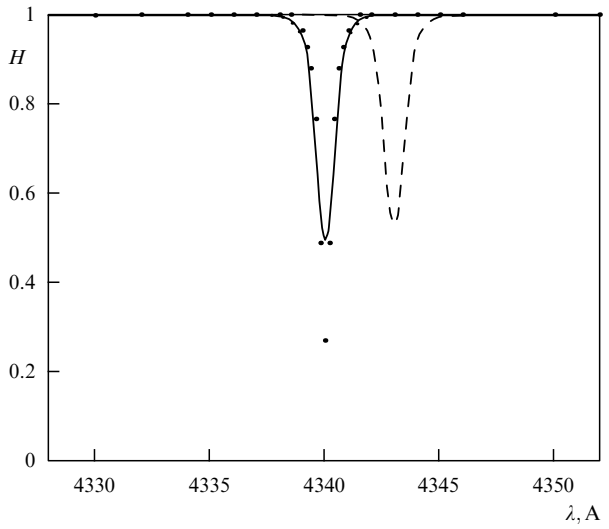

Figure 18. Theoretical profiles of the H_γ absorption line in the spectrum of X-ray Nova V404 Cyg synthesized for the orbital phase $\varphi = 0$ (the solid curve) and $\varphi = 0.25$ (the dashed curve). The points label the local line profile. A Doppler shift due to orbital motion of the star, as well as the entire star's rotational line broadening compared to the local profile are seen. The parameters are: $q = 17.143$, $m_v = 0.7M_\odot$, $m_x = 12M_\odot$, $\mu = 1$, $i = 56^\circ$, $\bar{T}_0 = 4500$ K, $P = 6^d.471$, $e = 0$, $k_x = 1$, $\kappa = 0.5$.

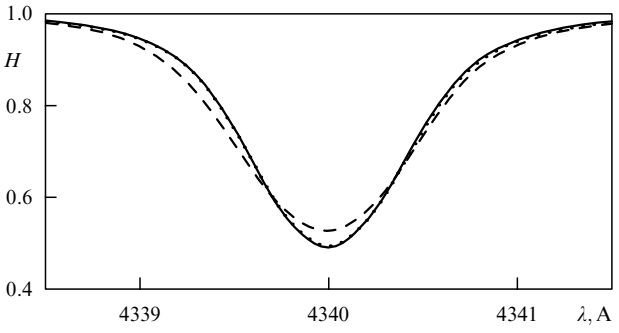

Figure 19. The effect of the optical star pear-like form on the shape of the absorption H_γ line profile in the spectrum of X-ray Nova V404 Cyg. Theoretical H_γ line profiles are synthesised for different orbital phases and reduced to a single central wavelength λ (Doppler shifts of the line caused by the orbital motion are subtracted). The solid curve corresponds to the phase $\varphi = 0$ (the X-ray source is behind the optical star), the dashed curve, to the phase $\varphi = 0.25$ (the star is seen from the side), and the dotted line corresponds to the phase $\varphi = 0.5$. This effect must be taken into account when deriving q from Eqn (36).

Thus, in contrast to the X-ray pulsar case, to determine black hole mass it is necessary to know two parameters: q and i which can be estimated from Eqns (32), (33), (35), and (36). Instead of the parameters q and i one may know the parameters m_v and i (the optical star mass can be approximately evaluated by its spectral class and luminosity class). Then the black hole mass m_x is derived from the solution to Eqn (24).

X-ray eclipses are not observed in none of ten known X-ray binaries containing black holes (excluding system XN Sco 1994). Therefore it appears impossible as yet to use Eqn (32) to estimate black hole mass. In this case one can only put some constraints on the parameters q, μ, i and masses m_x and

m_v using the condition of the X-ray eclipse absence [122]. So in the case of a black hole the most important point in determining its mass is a detailed quantitative interpretation of the optical light curve of the X-ray binary system (Eqn (33)) together with the use of information on the distance to the system (Eqn (35)) and spectroscopic information on the optical star axial rotation velocity (Eqn (36)). An additional control is to use the spectroscopic information on the spectral and luminosity class of the optical star, as well as information on the absence of X-ray eclipses. In addition, for X-ray Novae in quiescence one may put *a priori* $\mu = 1$ with a high confidence, since the stellar wind from low-mass F–M stars in these systems is negligibly small and an appreciable mass transfer from the F–M star onto a high-mass black hole may occur only when the F–M star fills fully its Roche lobe. Moreover, since during the mass transfer from the less massive F–M star onto the more massive black hole the distance between the binary system components increases and the nuclear time-scale of the K–M star is much larger than the cosmological time-scale and its radius increases negligibly small during the evolution, to maintain the mass transfer rate required, a mechanism of angular momentum loss should operate in the binary system connected with the radiation of gravitational waves and magnetic stellar wind [36, 37]. We also stress that for many X-ray Novae with black holes the observed value of the optical star mass function $f_v(m)$ exceeds 3 Solar masses. Then from expression (37) (see also inequality (25)) it follows that an absolute lower limit to the black hole mass exceeds 3 Solar masses regardless of specific parameters q, μ, and i.

Thus, the knowledge of the optical star mass function $f_v(m)$ together with the use of Eqns (33), (35), and (36) and all additional constraints described above provide us with the possibility to pose significant restrictions on the permissible region of the parameters q, μ, and i, which allows a reliable evaluation of either black hole mass or its lower limit from Eqn (37).

7. Specific systems

Characteristics of ten known X-ray binaries with black hole masses reliably estimated are listed in Table 2. We describe their most important features (for more detail see Ref. [41]).

7.1 Cyg X-1

This is a persistent X-ray binary system with a high-mass optical star - supergiant of spectral class O9.7 Iab. It is the first reliable black hole candidate [18, 122, 126]. Although the optical star mass function $f_v(m) = 0.23\,M_\odot$ [126, 127] is comparatively small here, it is tens times higher than $f_v(m)$ for the corresponding X-ray binaries with X-ray pulsars. No strictly periodic X-ray pulsations were discovered in Cyg X-1, only irregular X-ray intensity variability on a timescale as short as one millisecond [128] is observed in the 'low' state when the X-ray intensity is weak and the spectrum is hard and has a power-law shape (see, for example, Ref. [129]). In the 'high' state when the X-ray intensity is high and the spectrum is soft, the X-ray variability on the ultrashort timescale is not observed [129]. Mechanisms for the bimodal behaviour of accretion onto black holes and reasons for millisecond X-ray variability are discussed, for example, in Refs [130-132]. Note that before the discovery of the X-ray millisecond variability in Cyg X-1 [133] a possibility of such a variability was already justified in Ref. [134], where it was shown that characteristics of the ultrashort X-ray variability caused by rotation of 'hot spots' of accreting matter near the black hole would help in

Table 2. Characteristics of X-ray binary systems with black holes.

System	Optical star spectrum	Orbital period (days)	$f_v(m)$, $M_\odot$	m_x, $M_\odot$	m_v, $M_\odot$	L_x, erg s^{-1}	v_{pec}, km s^{-1}	Note
Cyg X-1 (V 1357 Cyg)	O9.7 Iab	5.6	0.23	7–18	20–30	$\sim 8 \times 10^{37}$	2.4±1.2	stab.
LMC X-3	B(3–6)II–III	1.7	2.3	7–11	3–6	$\sim 4 \times 10^{38}$	—	stab.
LMC X-1	O(7–9)III	4.2	0.14	4–10	18–25	$\sim 2 \times 10^{38}$	—	stab.
A0620−00 (V616 Mon)	K(5–7)V	0.3	3.1	5–17	∼0.7	$\leqslant 10^{38}$	-15 ± 5	trans.
GS 2023 + 338 (V404 Cyg)	K0IV	6.5	6.3	10–15	0.5–1.0	$\leqslant 6 \times 10^{38}$	8.5±2.2	trans.
GRS 1121−68 (XN Mus 1991)	K(3–5)V	0.4	3.01	9–16	0.7–0.8	$\leqslant 10^{38}$	26±5	trans.
GS 2000 + 25 (QZ Vul)	K(3–7)V	0.3	5.0	5.3–8.2	∼0.7	$\leqslant 10^{38}$	—	trans.
GRO J0422 + 32 (XN Per 1992 = V518 Per)	M(0–4)V	0.2	0.9	2.5–5.0	∼0.4	$\leqslant 10^{38}$	—	trans.
GRO J1655−40 (XN Sco 1994)	F5IV	2.6	3.2	4–6	∼2.3	$\leqslant 10^{38}$	-114 ± 19	trans.
XN Oph 1977	K3	0.7	4.0	5–7	∼0.8	$\leqslant 10^{38}$	38±20	trans.

Note: references to original papers see in the text. The peculiar radial velocities v_{pec} of the systems' barycentre are taken from Ref. [200].

discriminating against Schwarzschield and Kerr metrics of the black hole.

In paper [52] quasi-periodic oscillations of hard X-ray flux (QPO) from Cyg X-1 were discovered with the characteristic frequency of the order of a few hundredths Hz.

An analysis of the optical light curve of Cyg X-1 [18, 81 – 83, 135, 136], together with information on the distance to the source $d > 2$ kpc [122, 137], yields a lower limit of the black hole mass $m_x > 7M_\odot$. The optical star in Cyg X-1 is a supergiant of spectral class O9.7 Iab that is close to fill its Roche lobe. The binary system parameters uncertainty caused by the absence of X-ray eclipses (the angle i is estimated to lie within the interval $28^\circ - 63^\circ$) does not allow us to determine precisely the optical star Roche lobe filling factor ($\mu = 0.84 - 1.0$). However, irregular brightness decrease near maxima (see Fig. 7) evidences for possible eclipses of optical star by a variable accretion disc edge and of the disk by the star. This permits us to give preference to larger i from the permissible region ($i = 50^\circ$) and, correspondingly, to smaller μ ($\mu = 0.9$). Thus the analysis of the optical light curve of Cyg X-1 allows the determination of a reliable lower limit to the black hole mass ($m_x > 7M_\odot$) and provides the grounds to suppose that the optical star here is close to fill its Roche lobe but still underfills it ($\mu = 0.9$). This is in accordance with theory of evolution of massive close binary systems [36, 37].

A model of a triple system with neutron star for Cyg X-1 [138] is not confirmed by spectroscopic observations (see, for example, Ref. [139]). In addition, the stability of such a triple system and possibility of its keeping as a gravitationally bound system after the supernova explosion seem to be problematic.

The discovery of the 294-day precession period in X-ray and optical ranges [94, 95, 140] proves ultimately the reliability of the optical identification of the X-ray source Cyg X-1. We emphasise once again that for Cyg X-1 and all known high-mass compact X-ray sources (see below) neither X-ray pulsar nor Type I X-ray burster phenomena characteristic of accreting neutron star have been discovered.

7.2 LMC X-3

This is a persistent X-ray binary system with a comparatively high-mass optical star-giant of spectral class B(3–6) II-III. It is a reliable black hole candidate [141 – 143] since here $f_v(m) = 2.3M_\odot$ [141] and the confidence of the X-ray source identification with the optical star is proved by the discovery of a precession variability with a period of 198 days both in X-ray and optics [144]. No signatures of triplicity have been found [141].

The analysis of the optical light curve [142, 143] together with information on the absence of X-ray eclipses [145] and on the distance to the source $d = 55$ kpc, as well as spectroscopic information on absorption lines broadening in the optical star spectrum $v_{rot} \sin i = 130 \pm 20$ km s^{-1} [141, 143] enables us to give a reliable lower limit to the black hole mass $m_x > 7M_\odot$.

7.3 A0620–00

This is an X-ray Nova (transient X-ray binary system with a low-mass optical main-sequence star of spectral class K(5–7)V filling its Roche lobe). It is a very reliable black hole candidate since here $f_v(m) = 3.1M_\odot$ [146]. Thus, in this system the optical star mass function exceeds $3M_\odot$, an absolute upper limit to the neutron star mass predicted by the GR. The reliability of the optical identification is doubtless since together with the X-ray outburst an optical outburst was observed connected with the optical star and the accretion disc heating by a powerful X-ray radiation from an accreting black hole. A triple-system model with a neutron star is dismissed because no lines from the faint low-mass star K(5–7)V would be observed against the third massive star background light. The model of a massive laminar storaging disc around a neutron star [147] is also rejected, as the companion here is the low-mass K(5–7) main-sequence star with a normal chemical composition and not a helium remnant of an original massive star that should supply a lot of matter into the storaging disc. In the optical spectrum of A0620–00 the absorption line LiI 6707.8 A is discovered [148]. This line is also discovered in the spectrum of the black hole candidate V404 Cyg and of the X-ray binary with neutron star Cen X-4 [149]. As lithium is burnt out in thermonuclear reactions at the early stage of stellar evolution, to maintain an enhanced abundance of ^{7}Li in the K(5–7)V star's atmosphere this element should be generated by some mechanism. Such a mechanism could be the bombardment of the optical star surface by high energetic particles accelerated to relativistic velocities in the innermost parts of an accretion disc around a black hole or a neutron star. In particular, the reaction of collision of α-particles ($\alpha + \alpha = {}^7\mathrm{Li} + \mathrm{p} + \gamma$ (0.478 MeV)) could at least qualitatively explain the enhanced abundance of ^{7}Li seen in spectra of optical stars — components of X-ray Novae, as well as explain the origin and a relatively small width ($\Delta E/E \sim 0.1$) of an emission line near 0.5 MeV observed in the hard end of X-ray Novae spectra [149, 55, 59, 61, 62].

In paper [148], a rotational broadening of absorption lines in the optical star spectrum of A0620−00, $v_{rot} \sin i = 83 \pm 5$ km s^{-1}, is measured and the components mass ratio is determined (see expression (36)): $1/q = 0.067 \pm 0.01$ ($q = 15$). The error of q caused by the use of (36) based on the substitution of a tidally-distorted star by an equal-volume sphere does not exceed 5% [148]. The orbit inclination i for the given q is evaluated by means of the interpretation of the optical and infrared light curves formed mainly by the optical star K(5–7)V star ellipticity effect [148, 150, 151] under the absence of X-ray eclipses. This yields a reliable black hole mass estimate $m_x = (5–17)M_\odot$ [151].

The optical and infrared light curves of A0620–00 exhibit unequal heights of maxima and show a long-term variability on timescales of about one year [152, 153]. This variability could be explained by the contribution of the emission from an elliptic accretion disc with a hot spot at its outer boundary with a turning major semiaxis [91, 92]. However, as became clear in the last time from the analysis of spectrophotometric measurements, the accretion disc and hot spot contribution into the total optical luminosity of the system is fairly small (about 6% near the line H_α 6563A and decreases in the infrared part of the spectrum nearly at 2.2 μm) [148, 151]. As the optical star light in A0620–00 prevails, it appears more natural to explain the long-term optical and infrared variability of A0620–00 by the appearance, motion and disappearance of spots on the K(5–7)V star surface [80].

7.4 GS 2023 + 338 (V404 Cyg)

This is an X-ray Nova with an optical star of spectral class K0 IV (a 'naked giant' filling its Roche lobe after having lost a significant part of its mass due to mass transfer onto the neighbour relativistic object). This is a unique system in

having the optical star mass function $f_v(m) = (6.3 \pm 0.3)M_\odot$ (!) [154]. It is the most reliable black hole candidate. In the optical star spectrum the absorption line of Li 6707.8 A is discovered [155]. The orbital period of the system is unusually large for X-ray binaries of such a class ($P = 6.47$ days). There are also evidences for spectral and photometric variability of the system with a period of 0.24 days of so far unclear nature [156]. The optical light curve of V404 Cyg, demonstrating the ellipticity effect with brightness minima coinciding with the moments of the radial velocity curve crossing the γ-velocity, is obtained in Ref. [157]. This provides a reliable justification to the model of a binary system with the period of 6.47 days [157]. The ellipticity effect is confirmed in Refs [158, 159] in which infrared J and K light curves of V404 Cyg are obtained.

In paper [160] a rotational broadening of absorption lines in the optical star K0 IV spectrum is obtained: $v_{\rm rot} \sin i = 39.1 \pm 1.2$ km s^{-1}. The corresponding mass ratio of the components (see expression (36)) is $1/q = 0.060 \pm 0.004$ ($q = 17$). The analysis of the infrared K-light curve of V404 Cyg dominated by the ellipticity effect yields the estimation $i = 52^\circ - 60^\circ$ [159]. With the parameters q and i found the black hole mass is $(10 - 15)M_\odot$ [159, 160]. Thus, in V404 Cyg the relativistic object mass is more than three times higher than $3M_\odot$ — an absolute upper neutron star mass limit predicted by the GR (!).

7.5 GRS 1121-68 (XN Mus 1991)

This is an X-ray Nova with a main-sequence optical star of spectral class K(0–4)V that fills its Roche lobe. It was discovered independently from GRANAT and GINGA satellites in January 1991 [161 – 163]. The X-ray Nova was identified with the optical Nova Muscae ($V = 13$ during the outburst) in Refs [164, 165]. According to the recent spectral and photometric observations of XN Mus 1991 in quiescence [166], the orbital period of this transient X-ray binary system is 0.433 days, the optical star K(0–4)V mass function is $f_v(m) = (3.07 \pm 0.4)M_\odot$. In paper [167], more precise mass function $f_v(m) = (3.01 \pm 0.15)M_\odot$ is given. The I light curve represents a double wave over the orbital period which is characteristic of the ellipticity effect. The brightness minima correspond to the optical star radial velocity curve crossing the γ-velocity, which confirms a binary system model and proves the correctness of the mass function $f_v(m)$ determination. The orbit of the system is circular.

The binary system's parameters estimation from the infrared I light curve and the radial velocity curve [84, 166] leads to the following results: $i = 39^\circ - 43^\circ$, $m_v = (0.7 - 0.8)M_\odot$ (the latter is postulated according to the optical star spectral class and luminosity class), $q = 12 - 21$, and $m_x = (9 - 16)M_\odot$. Thus we conclude that XN Mus 1991 is a reliable black hole candidate.

Paper [61] reported on the discovery of a variable, comparatively narrow ($\Delta E/E \sim 0.1$) emission line in the XN Mus 1992 X-ray spectrum near 0.5 MeV, which may be connected with electron–positron plasma annihilation or with other mechanisms (see above).

7.6 GS 2000 + 25 (QZ Vul)

This is an X-ray Nova with a main-sequence optical star of spectral class K(3–7)V filling its Roche lobe. The X-ray and corresponding optical outbursts were registered in 1988 [168 – 170]. By 1989 the brightness decreased from $V = 16.4$ during the outburst to $R = 21.2$, so that in the quiescent state QZ Vul is one of the faintest optical objects of the known X-ray Novae. The orbital period is $P = 0.344092$ days [118]. In paper [118] the optical star mass function in QZ Vul was measured: $f_v(m) = (5.02 \pm 0.46)M_\odot$.

This is the second highest mass function after V404 Cyg. From the condition of the absence of X-ray eclipses one may restrict the orbit inclination $i < 80^\circ$. Hence, by setting the quantity $m_v = 0.7M_\odot$ according to the spectral and luminosity classes of the K(3–7)V optical star, one may estimate the black hole mass $m_x > (5.8 \pm 0.5)M_\odot$ [118]. On the other hand, in paper [171], based on the analysis of the infrared I-light curve of QZ Vel caused mainly by the ellipticity effect, the bound $i \geqslant 67^\circ$ is obtained. With these data, the black hole mass is estimated to be $m_x = (5.3 - 8.2)M_\odot$ [118]. Thus, the system QZ Vul is a very reliable black hole candidate.

7.7 GRO J1655–40 (XN Sco 1994)

This is an X-ray Nova with a comparatively low-mass optical giant star of spectral class F5 IV filling its Roche lobe. It is an eclipsing binary system with the orbital period $p = 2^d{,}63$. In paper [172] the optical star mass function is measured to be $f_v(m) = 3.2M_\odot$ which exceeds the neutron star mass upper limit. The mass of the F5 IV optical star estimated by means of its spectral class and luminosity class is $\sim 2.3M_\odot$. Since i is close to 90°, which follows from the presence of eclipses, the black hole mass is estimated as $(4–6)M_\odot$. Thus, the X-ray Nova XN Sco 1994 is also a reliable black hole candidate.

7.8 XN Oph 1977

This is an X-ray Nova with a low-mass optical star K3 filling its Roche lobe. The orbital period is $0^d{.}7$, the amplitude of ellipticity effect in the R-band is $\sim 0^m{.}2$ [125]. The optical star mass function $f_v(m) = (4.0 \pm 0.8)M_\odot$ is measured in Ref. [173] providing an evidence for a black hole existence in this system. The estimate of i from the light curve is $i = 60^\circ - 80^\circ$. The black hole mass is evaluated to be $m_x = (6 \pm 1)M_\odot$.

7.9 GRO J0422 + 32 (XN Per 1992 = V518 Per)

This is an X-ray Nova with a low-mass optical star of the main sequence of spectral class M(0–4)V that fills its Roche lobe. It was discovered by the GRO in 1992 [174]. The discovery of the optical outburst was reported in [175]. The X-ray outburst was confirmed by observations from MIR-KVANT and GRANAT space observatories [176], which also revealed the absence of the soft X-ray component corresponding to a low-energetic state. In this state a power-law 'tail' is observed in the X-ray spectrum up to energies of 1 – 2 MeV. The optical light curve during the outburst revealed a very slow brightness decay and the presence of mini-outbursts during the subsequent 18 months [177]. The system is very faint in quiescence ($V = 22.4$) [178]. The discovery of optical variability caused by the optical star ellipticity [179] made it possible to finally determine the orbital period to be $P = 0,212265$ days. The optical star M(0–5)V mass function $f_v(m) = (0.85 \pm 0.30)M_\odot$ was measured in Refs [180, 181]. The optical star light contribution into the total optical luminosity of the system is $(35 \pm 6)\%$ in the region $\lambda = 6000 - 6500$ A and $(52 \pm 8)\%$ in the region $\lambda = 6700 - 7500$ A [181]. The remaining part of the optical luminosity is due to the contribution from the accretion disc together with a hot spot at its outer boundary.

By setting the M(0–4)V optical star mass $m_v = 0.4M_\odot$ in accordance with its spectral and luminosity classes, as well as by deriving the orbit inclination $i = 30^\circ - 35^\circ$ from the analysis of the infrared I light curve (with account of the

ellipticity effect and the accretion disc contribution $\lesssim 48\%$), the authors of Ref. [181] estimated the relativistic object mass in V518 Per: $m_x = (2.5-5.0)M_\odot$. Thus, the relativistic object in XN Per may be considered a comparatively low-mass black hole with a mass of about $4M_\odot$.

7.10 LMC X-1

This is a persistent X-ray binary system with a high-mass optical giant star of spectral class O(7–9)III. The mass function of the optical star as measured by its absorption lines is $f_v(m) = 0.14M_\odot$ [182]. The relativistic object mass estimate $m_x \geqslant 4M_\odot$ is obtained in Ref. [182] using information on the distance to the system $d = 55$ kpc and the radial velocity curve measured by emission lines, in particular, HeII 4686 A line formed in the vicinity of the relativistic object. Thus, in LMC X-1 a comparatively low-mass black hole ($\sim 4M_\odot$) exists, and in this respect it is similar to XN Per 1992 = V518 Per. It should be noted that the optical stars in LMC X-1 and V518 Per are radically different.

7.11 Other systems

Binary systems SS433 and HD 197406 were considered as the black hole candidates in Ref. [183]. The analysis of optical eclipses in SS433 [102] leads to the estimation of the mass ratio of the components $q = m_x/m_v > 0.25$. On the other hand, the analysis of X-ray eclipses in SS433 [184] enables us to obtain the estimate $q < 0.25$. Thus, estimates of q obtained from optical and X-ray data are overlapped at $q = 0.25$. With this value of q and using the relativistic object mass function derived from the analysis of HeII 4686A emission line, $f_x(m) = 10.1M_\odot$ [185], we obtain the relativistic object mass $m_x = 4M_\odot$, which favours the presence of a black hole in SS433 binary system [102]. Note that the large $f_x(m)$ for SS433 is confirmed by observations obtained with the 6-meter telescope of the Special Astrophysical Observatory [186]. At the same time, a small value $f_x(m) = 2M_\odot$ is obtained in Ref. [187] on the basis of new spectroscopic observations of the HeII 4686A emission in SS433. At $q = 0.25$ this corresponds to masses $m_x = 0.8M_\odot$ and $m_v = 3.2M_\odot$. With such characteristics the system SS433 becomes an analogue to the X-ray binary system HZ Her containing a moderate-mass optical star and a neutron star. In this case it is difficult to explain a huge luminosity of the optically-bright accretion disc ($\sim 10^{39}-10^{40}$ erg s^{-1}) and a high mass-loss rate from the optical star ($M \approx 10^{-4}M_\odot$ /yr). It should be noted, however, that the spectroscopic observations [187] were taken at the precession period phases not close to the moment of the maximum separation of moving emissions in the SS433 spectrum. As shown in Ref. [186], it is at the phases of moving emissions maximum separation (when the accretion disc is maximum open to a terrestrial observer) that the mass function $f_x(m)$ for SS433 is maximal. Thus, the problem of the black hole existence in the system SS433 still waits for its ultimate solution until new high-resolution spectroscopic observations taken at phases of the maximum separation of moving emissions will become available. Therefore the object SS433 is not included by us into the list of black hole candidates.

The binary system of Wolf–Rayet type HD197406 of spectral type WN7 with a period of ~ 4.3 days and a very large height over the galactic plane of ~ 1 kpc was mentioned as a black hole candidate in Ref. [188]. The main arguments favouring the presence of a black hole in this system is its large height over the plane of the Galaxy, which may be connected with a kick the binary system acquired after the Supernova explosion, as well as the invisibility of lines from a massive ($m_x \geqslant 5M_\odot$) companion. As became clear in the last time, the X-ray luminosity of the HD197406 in the "Einstein" X-ray observatory range (0.2 – 4) keV does not exceed 10^{32} erg s^{-1}, which is too low for an accreting relativistic object. This conclusion relates also to other suspected binary systems of Wolf–Rayet type with relativistic companions. Therefore we have not considered HD197406 as a black hole candidate. However, the possibility of the existence of X-ray binaries containing a Wolf–Rayet star as a donor is proved by the recent discovery of a Wolf–Rayet star in the well-known short-period X-ray binary system Cyg X-3 [189]. By its characteristics (mass, radius, and effective temperature) the Wolf–Rayet star in Cyg X-3 corresponds well to the model of a helium remnant formed after the mass loss from an originally high-mass star [190]. Therefore the searches for black holes in binary systems containing Wolf–Rayet stars as optical components represent an actual task.

We have not considered also some other candidates to black holes of GX 339-4 type for which no mass estimates are known as yet but which are selected by indirect features [54, 56, 191, 192], such as the presence of two levels of the X-ray emission with strongly different spectra: a relatively soft X-ray spectrum at the high state, the presence of a power-law 'tail' in the spectrum extending up to energies of 1 – 2 MeV at the low state, fast irregular X-ray intensity fluctuations, etc. As already noted, in our review we restrict ourselves to considering black holes with reliable mass estimates.

8. Discussion of the results

To date, the number of reliable black hole candidates amounts to ten. Seven of them (Cyg X-1, LMC X-3, A0620–00, V404 Cyg, XN Mus 1991, QZ Vul, XN Sco 1994) have an uppermost reliability priority in mass determination. The mass determination reliability is guaranteed by the following points.

First, the joint use of the optical star radial velocity curve and optical light curve caused mainly by the ellipticity effect [18, 19], allows a firm justification of the binary system model and of the correctness of the optical mass function $f_v(m)$ determination. In particular, in the case of circular or almost circular orbits, the transition of the optical star radial velocity curve through the γ-velocity at the moments of brightness minima proves the fact that the radial velocities measured reflect the orbital motion of the optical star and not the motion of gaseous streams within the system or pulsations of the star. The example of the binary system SS433 where the initially-derived mass function measured by the stationary H_α emission line [193] turned out to be not corresponding to reality since this line is formed in a gaseous stream [86], illustrates the importance of the joint interpretation of the radial velocity curve and the optical light curve [86, 185].

Second, for many X-ray binary systems from Table 2 the measured optical star mass functions $f_v(m)$ already exceed $3M_\odot$, which without any additional modelling of the binary system allows us to make a conclusion that the relativistic object mass exceeds an upper limit of the neutron star mass predicted by the GR. The availability of the effective methods to estimate the parameters i and q, based on the analysis of the optical or infrared light curve dominated by the optical star ellipticity and on the spectroscopic measurement of the rotational broadening of lines in the optical star spectrum,

allows us to estimate reliably the relativistic object mass or its lower limit by means of the optical mass function $f_v(m)$ observed (see expression (37)). An additional control of the reliability of the estimation of m_x is provided by information on the absence of X-ray eclipses, by information on the distance to the system, as well as by information on the optical star mass m_v evaluated from its spectral class and luminosity class.

Therefore, to date the problem of stellar-mass black holes has acquired a firm observational basis. The recent direct dynamic mass determinations of active galactic nuclei M87 ($2.4 \times 10^9 M_\odot$) and NGC 4258 ($3.6 \times 10^7 M_\odot$) [194, 195] allow us to make the same statement concerning supermassive black holes.

In Figure 20 we plot the relativistic object masses as a function of companion masses in binary systems. The companions to X-ray pulsars and black holes in binaries are optical stars of spectral class M–O. The companions to binary radiopulsars are inactive neutron stars (PSR 1913+16, PSR 2127+11C, PSR 1534+12), white dwarfs (for example, PSR 1855+09), as well as high-mass stars of spectral class $\sim$ B (for example, PSR 1259–63). We do not deal here with planets — companions to radiopulsars. The masses of binary radiopulsars are determined with a high precision by means of relativistic effects in their orbital motion (see, for example, Refs [106, 107, 196–198], as well as a catalogue [31]). As seen from Fig. 20, no dependence of the relativistic object mass on the companion mass exists. Both neutron stars and black holes happen in binary systems with companions of both high and low mass. The situation here is similar to classical close binaries in which any combination of components happen (see, for example, [199]). Based on the data from Table 2, there are serious grounds to believe that among black holes in binary systems both high-mass objects (V404 Cyg, $m_x = (10-15)M_\odot$) and low-mass objects (V518 Per, $m_x = (2.5-5.0)M_\odot$) occur.

A very important observational fact should be emphasised. In any case when the mass of an X-ray or radiopulsar has become available (there are 11 such measurements), it does not exceed $(2–3)M_\odot$ and is $\sim 1.4M_\odot$ on average. At the same time, as already noted, in none of ten high-mass ($m_x > 3M_\odot$) X-ray sources — black hole candidates the phenomena of X-ray pulsar or Type I X-ray burster characteristic of accreting neutron stars have been discovered. This fact has a fundamental meaning and may be considered as an observational argument favouring that the ten black hole candidates observed are indeed black holes. Of course, the fact of the absence of X-ray pulsations or Type I X-ray bursts cannot be considered as a final proof that the high-mass X-ray sources listed in Table 2 belong to black holes in the sense of the GR, as the absence of pulsations and bursts is only a necessary but not a sufficient test of the black hole existence. Since the black hole problem became now an observational one, the search for the sufficient observable criteria of black holes seems to be very important. In this connection it seems promising to study accreting black holes in binary systems in hard X-rays and gamma-rays (see, for example, Refs [55, 59, 61, 62]), as well as to observe collimated

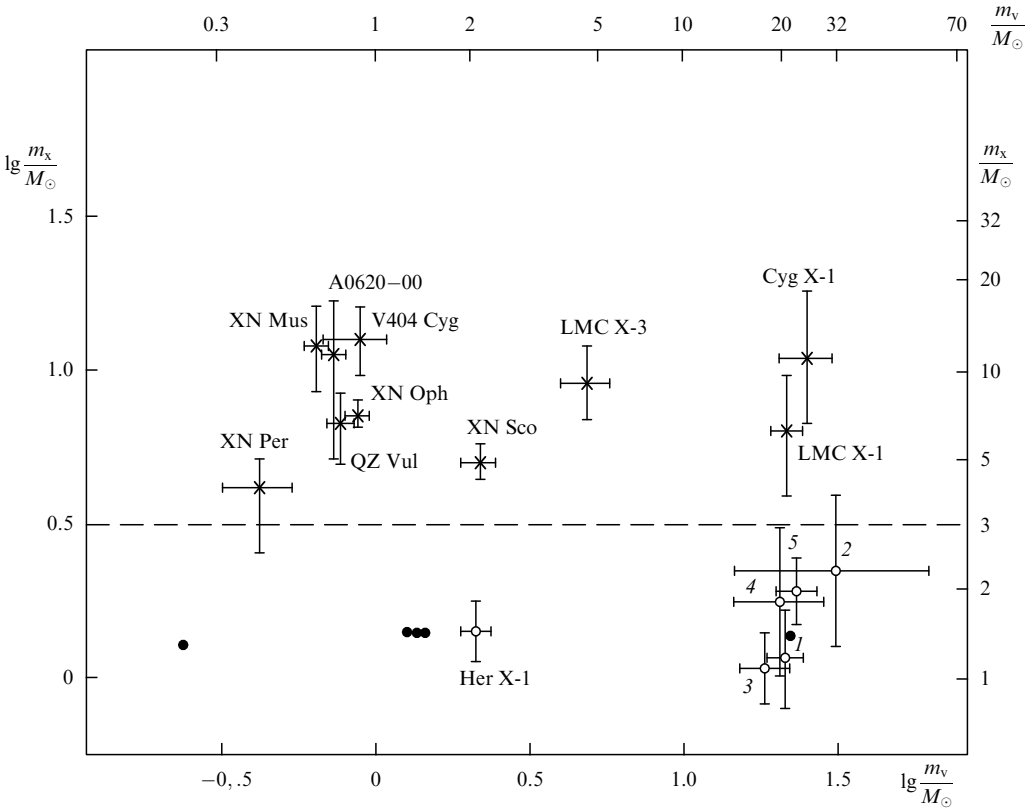

Figure 20. The dependence of neutron star masses m_x (points and circles) and black hole masses (crosses) on the companion's masses m_v in close binary systems. The figures label: *1* — Cen X-3, *2* — LMC X-4, *3* — SMC X-1, *4* — 4U1538-52, *5* — 4U0900–40. The error bars in mass determination are shown for X-ray pulsars (circles). The mass determination errors for radiopulsars (points) are negligibly small. None of the massive ($m_x > 3M_\odot$) X-ray sources belongs to either an X-ray pulsar or a Type I X-ray burster, i. e., displays the signatures characteristic of accreting neutron stars.

relativistic jets with velocities $\sim 0.9c$ from accreting black holes in binary systems [64 – 66].

As seen from Table 2, in the cases where the companion is a hot optical star of spectral class O–B (Cyg X-1, LMC X-3, LMC X-1), the X-ray source is persistent. In all systems with low-mass cool companions of late spectral classes M-F (A0620–00, V404 Cyg, XN Mus, QZ Vul, XN Sco 1994, XN Oph 1977, XN Per 1992) the X-ray source is transient (an X-ray Nova). Then in quiescence when the X-ray source luminosity $L_x \leqslant 10^{33}$ erg s^{-1}, in optical spectra strong emission lines of hydrogen are observed indicative of a disc-like envelope localised around a relativistic object, as well as of a hot spot in the site of the encounter of the gaseous stream from the optical star with the outer disc edge (see, for example, Refs [91, 92, 118]). These facts evidence that the optical stars in the transient X-ray binary systems — X-ray Novae — fill their Roche lobes ($\mu = 1$) and the disc-like envelopes around relativistic objects in quiescence represent here most likely storaging discs with an extremely low viscosity, which causes a very low accretion rate and X-ray luminosity. The activity of the optical M–F star with a convective envelope may serve as a trigger to turn on some mechanism of the disc viscosity growth (for example, the development of turbulence), which may explain the X-ray Nova phenomenon [80]. Another feature of the X-ray Novae is a very high component mass ratio $q = 10-20$ at which the accretion disc around the relativistic object has a large relative size. Possibly, this point is also important for forming the storaging disc and triggering different instability inside it. For high-mass hot O–B stars the envelopes are in the radiative equilibrium, their surface activity is low and, in addition, the mass ratio in the X-ray binary systems with O–B companions is of the order of unity. This probably underlies the fact that X-ray sources in Cyg X-1, LMC X-3 and LMC X-1 are persistent. Theoretically, these questions are poorly elaborated as yet (see in this connection Refs [200 – 203]).

The evolution of high-mass binary systems with mass exchange up to the stage the relativistic object formation is studied in Refs [36, 37]. The evolutionary aspects of the problem of black holes in binary systems are considered in Refs [23, 183, 204]. The condition for a binary system to survive as gravitationally-bound at late evolutionary stages may be written in the form [23]:

$$0.1m_0^{1.4} - m_v < 2m_x\,, \tag{38}$$

where $0.1m_0^{1.4}$ is the mass of the helium exploding star after the mass exchange in a binary system, m_0 is the initial mass of a hydrogen-helium main-sequence star, m_x is the mass of a relativistic object remained after the supernova explosion, m_v is the mass of the optical star in the X-ray binary system. For V404 Cyg where $m_x > 6.3M_\odot$ and $m_v \approx 1M_\odot$, from relationship (38) we find $m_0 \leqslant 32M_\odot$. For A0620–00 where $m_x > 3M_\odot$, we obtain $m_0 \leqslant 21M_\odot$. Therefore, at least in the case of the X-ray Novae, in order to form a comparatively high-mass black hole, it is not necessary to consider galactic stars of the highest mass $(50-100)M_\odot$ as their progenitors. The mixing of stellar interiors at late evolutionary stages can help in forming high-mass (with a mass of order $10M_\odot$) black holes [183]. The evolution of the transient X-ray binaries with low-mass optical companions is hard to understand without involving the model with a common envelope [205, 206] or model of a triple system [207, 208]. For further detail on the evolutionary aspects of X-ray binaries see, for example, Refs [209 – 212].

9. Conclusion

In our review we described astronomical methods and results of the black hole mass determination in X-ray binary systems based mainly on their optical studies. The results obtained in this field have a great meaning for fundamental physics and relativistic astrophysics, as well as for theory of internal structure and evolution of stars. It may be said without exaggeration that in the problem of searching for and observational studies of black holes a 'quiet' revolution has occurred in the last years and the problem of black holes in the Universe became an observational one. This undoubtedly means a qualitatively new stage of black hole studies and must lead to a significant progress in this field of science. Already now we may conclude, based on a great number of neutron star and black hole mass determinations, that observations of relativistic objects in binary stellar systems conform with the predictions of A Einsten's General Relativity.

The author thanks V L Ginzburg, R A Sunyaev and M R Gilfanov for valuable notes.

The work was supported by the Russian Fund for Basic Research and the Cosmomicrophysics Centre "Kosmion"

References

1. Zeldovich Ya B *Dokl. Akad. Nauk SSSR.* **155** 67 (1964) [*Sov. Phys. Dokl.* **9** 195 (1964)]
2. Salpeter E E *Astrophys. J.* **140** 796 (1964)
3. Ginzburg V L *On Physics and Astrophysics* (Moscow: Bureau Kvantum, 1995) p. 112
4. Novikov I D, Frolov V P *Fizika Chernykh Dyr* (The Black Hole Physics) (Moscow: Nauka, 1986) p. 6
5. Novikov I D, Zeldovich Ya B *Nuovo Cimento Suppl.* **4** 810 (1966)
6. Zeldovich Ya B, Guseynov O H *Astrophys. J.* **144** 840 (1966)
7. Trimble V, Thorne K S *Astrophys. J.* **156** 1013 (1969)
8. Schvartzman V F *Astron. Zh.* **48** 479 (1971)
9. Blondin J M *Ashrophys. J.* **308** 755 (1986)
10. Park M-G *Astrophys. J.* **354** 64 (1990)
11. Shakura N I *Astron. Zh.* **49** 921 (1972) [*Sov. Astron.* **16** 756 (1973)]
12. Shakura N I, Sunyaev R A *Astron. Astrophys.* **24** 337 (1973)
13. Pringle J E, Rees M J *Astron. Astrophys.* **21** 1 (1972)
14. Novikov I D, Thorne K S, in *Black Holes* (Eds C De Witt, B S De Witt) (London: Gordon and Breach, 1973) p. 343
15. Forman W et al. *Astrophys. J. Suppl.* **38** 357 (1978)
16. Cherepashchuk A.M et al. *Inform. Bull. Var. Stars* (720) (1972)
17. Bahcall J N, Bahcall N A *Astrophys. J. Lett. Ed.* **178** L1 (1972)
18. Lyutyi V M, Syunyaev R A, Cherepashchuk A M *Astron. Zh.* **50** 3 (1973) [*Sov. Astron.* **17** 1 (1973)]
19. Lyutyi V M, Syunyaev R A, Cherepashchuk A M *Astron. Zh.* **51** 1150 (1974)
20. Lamb F K, in *Frontiers of Stellar Evolution* (Ed. D L Lambert) (Astron. Soc. of the Pacific, 1991) p. 299
21. McClintock J E, in *X-Ray Binaries and Recycled Pulsars* (Eds E P J Van den Heuvel, S A Rappoport) (Dordrecht–London: Kluwer, 1992) p. 27
22. Cowley A P *Ann. Rev. Astron. Astrophys.* **30** 287 (1992)
23. Tutukov A V, Cherepashchuk A M *Astron Zh.* **70** 307 (1993)
24. Novikov I D, in *Key Problems in Astronomy, Tenerife 1995*
25. Shapiro S, Teukolsky S *Chernye dyry, belye karliki i neĭtronnye zvezdy* (Black Holes, White Dwarfs and Neutron Stars) (Moscow: Mir, 1985) [Translated into English (J.Wiley and Sons, 1983)]
26. Kopal Z *Close Binary Systems* (New York: Wiley, 1959)
27. Taam R E, Fryxell B A *Astrophys. J. Lett. Ed.* **327** L73 (1988)
28. Blondin J M et al. *Astrophys. J.* **356** 591 (1991)
29. Livio M et al. *Mon. Not. Roy. Astron. Soc.* **253** 633 (1991)
30. Ishii T et al. *Astrophys. J.* **404** 706 (1993)
31. Bisikalo D V, Boyarchuk A A, Kuznetzov O A et al. *Astron. Reports* **71** 560 (1994)
32. Davidson K, Ostriker J P *Astrophys. J.* **179** 585 (1973)
33. Illarionov A F, Sunyaev R A *Astron. Astrophys.* **39** 185 (1975)

34. Kolykhalov P I, Syunyaev R A *Pis'ma Astron. Zh.* **5** 338 (1979)
35. Bondi H, Hoyle F *Mon. Not. Roy. Astron. Soc.* **104** 273 (1944)
36. Tutukov A V, Yungelson L R *Nauchnye Informatsii Astrosoveta Akad. Nauk SSSR* **27** 58 (1973)
37. Van den Heuvel E P J, in *Structure and Evolution of Close Binary Systems* (Eds P Eggleton, S Mitton, J Whelan) (Dordrecht: Reidel, 1976) p. 35
38. Margon B *Ann. Rev. Astron. Astrophys.* **22** 507 (1984)
39. Cherepashchuk A M *Sov. Sci. Rev. Astrophys and Space Phys.* **7** 1 (1988)
40. Aslanov A A et al. *Katalog tesnykh dvoĭnykh zvezd na pozdnikh stadiyakh évolyutsii* (The Catalog of Close Binary Stars at Late Evolutionary Stages) (Ed. A M Cherepashchuk) (Moscow: Izdatel'stvo MGU, 1989)
41. Cherepashchuk A M et al. *Highly Evolved Close Binary Stars: Catalog* (Ed. A M Cherepashchuk) (London: Gordon and Breach, 1996)
42. Schreier E et al. *Astrophys. J. Lett. Ed.* **172** L79 (1972)
43. Lamb F K, Pethick C J, Pines D *Astrophys. J.* **184** 271 (1973)
44. Basko M M, Sunyaev R A *Mon. Not. Roy. Astron. Soc.* **175** 395 (1976)
45. Lipunov V M *Astrofizika neĭtronnykh zvezd* (Astrophysics of Neutron Stars) (Moscow: Nauka, 1987) [Translated into English (Berlin: Springer-Verlag, 1992)]
46. Gnedin Yu N, Sunyaev R A *Astron. Astrophys.* **36** 379 (1974)
47. Bisnovatyi-Kogan G S *Astron. Zh.* **50** 902 (1973) [*Sov. Astron.* **18** 574 (1974)]
48. Grindlay J E et al. *Astrophys. J. Lett. Ed.* **205** L127 (1976)
49. Maraschi L, Cavaliere A *Highlight in Astronomy* (Ed. E A Müller) (Dordrecht: Reidel, 1977) p. 127
50. Joss P C, Rappoport S A *Ann. Rev. Astron. Astrophys.* **22** 537 (1984)
51. Ebisawa K, Mitsuda K, Inoue H *Publ. Astron. Soc. Jpn.* **41** 159 (1989)
52. Vikhlinin A et al. *Astrophys. J.* **424** 395 (1994)
53. Van der Klis M et al. *Nature* (London) **316** 225 (1985)
54. Tanaka Y, Lewin W H G, in *X-Ray Binaries* (Eds W H J Lewin et al.) (Cambridge: Cambridge Univ. Press, 1995) p. 126
55. Sunyaev R A et al. *Astron. Astrophys.* **247** L29 (1991)
56. Gilfanov M et al., in *Frontiers Science Series № 12, New Horizon of X-Ray Astronomy* (Eds F Makino, T Ohashi, 1994) p. 433
57. Tanaka Y, in *Proc. 23rd ESLAB Symp.* (Eds J Hunt, B Battrick) (ESA Publications Division, 1989) Vol. 1, p. 3
58. Ebisawa K et al. *Publ. Astron. Soc. Jpn.* **46** 375 (1994)
59. Gilfanov M et al., in *NATO ASI Series. Series C., The Lives of Neutron Stars* (Eds A Alpar, U Kiziloglu, J Van Paradijs) (Dordrecht: Kluwer, 1995) p. 331, 450
60. Gilfanov M et al. *Astron. Astrophys. Suppl.* **97** 303 (1993)
61. Sunyaev R et al. *Astrophys. J. Lett. Ed.* **389** L75 (1992)
62. Gil'fanov M et al. *Pis'ma Astron. Zh.* **17** 1059 (1991)
63. Sunyaev R et al. *Astrophys. J. Lett. Ed.* **383** L49 (1991)
64. Mirabel I et al. *Nature* (London) **358** 215 (1992)
65. Mirabel I, Rodriguez L *Nature* (London) **371** 46 (1994)
66. Hjellming R, Rupen M *Nature* (London) **375** 464 (1995)
67. White N E, Marshall F E *Astrophys. J.* **281** 354 (1984)
68. Syunyaev R A et al . *Pis'ma Astron. Zh.* **17** 975 (1991)
69. Martynov D Ya *Zatmennye peremennye zvezdy* (Eclipsing Binary Stars) (Moscow: Nauka, 1971) p. 313
70. Martynov D Ya *Zvezdy i zvezdnye sistemy* (Stars and Stellar Systems) (Moscow: Nauka, 1981) p. 9
71. Avni Y *Astrophys. J.* **209** 574 (1976)
72. Subbotin M F *Kurs nebesnoĭ mekhaniki* (Course of Celectial Mechanics) Vol. 2 (Moscow: Gosteorizdat, 1945) p. 223
73. Zeipel H v *Mon. Not. Roy. Astron. Soc.* **84** 665, 684, 702 (1924)
74. Lucy L B *Z. Astrophys* **65** 89 (1967)
75. Sobolev V V *Kurs teoreticheskoj astrofiziki* (Course of Theoretical Astrophysics) (Moscow: Nauka, 1967) p. 83
76. Goncharskiĭ A V, Romanov S Yu, Cherepashchuk A M *Konechno-parametricheskie obratbye zadachi astrofiziki* (Finite-parametric Inverse Problems in Astrophysics) (Moscow: Izdatel'stvo MGU, 1991) p. 83
77. Bochkarev N G et al. *Pis'ma Astron. Zh.* **5** 185 (1979)
78. Kemp J C et al. *Astrophys. J. Lett. Ed.* **220** L123 (1978)
79. Dolginov A Z, Gnedin Yu N, Silant'ev N A *Rasprostranenie i polyarizaciya izlucheniya v kosmicheskoi srede* (Propagation and Polarization of Radiation on Cosmic Medium) (Moscow: Nauka, 1979) p. 180
80. Khruzina T S, Cherepashchuk A M *Astron. Zh.* **72** 203 (1995)
81. Balog N I, Goncharskiĭ A V, Cherepashchuk A M *Astron. Zh.* **58** 67 (1981) [*Sov. Astron.* **25** 38 (1981)]
82. Balog N I, Goncharskiĭ A V, Cherepashchuk A M *Pis'ma Astron. Zh.* **7** 605 (1981)
83. Nadjip A E et al. *Astron. Zh.* **73** (1996)
84. Antokhina E A, Cherepashchuk A M *Pis'ma Astron. Zh.* **19** 500 (1993)
85. Basko M M, Sunyaev R A *Astrophys. Space Sci.* **23** 117 (1973)
86. Cherepashchuk A M *Mon. Not. Roy. Astron. Soc.* **194** 761 (1981)
87. Cherepashchuk A M *Astron. Zh.* **52** 833 (1975)
88. Bisnovatyi-Kogan G S et al. *Astron. Zh.* **54** 241 (1977) [*Sov. Astron.* **21** 133 (1977)]
89. Petterson J A *Astrophys. J. Lett. Ed.* **201** L61 (1975)
90. Gerend D, Boynton P E *Astrophys. J.* **209** 562 (1976)
91. Haswell C A, Robinson E L, Horne K D, in *Accretion Powered Compact Binaries* (Ed. C W Mauche) (Cambridge: Cambridge Univ. Press, 1990) p. 17
92. McClintock J E, Remillard R A *Astrophys. J.* **350** 386 (1990)
93. Khruzina T S, Cherepashchuk A M *Astron. Zh.* **59** 512 (1982) [*Sov. Astron.* **26** 310 (1982)]
94. Priedhorsky W C, Terrell J, Holt S S *Astrophys. J.* **270** 233 (1983)
95. Kemp J et al. *Astron. Zh.* **64** 326 (1987) [*Sov. Astron.* **31** 170 (1987)]
96. Cowley A P et al. *Astrophys. J.* **381** 526 (1991)
97. Roberts W J *Astrophys. J.* **187** 575 (1974)
98. Cherepashchuk A M *Pis'ma Astron. Zh.* **7** 201 (1981)
99. Whitehurst R *Mon. Not. Roy. Astron. Soc.* **232** 35 (1988)
100. Charles P A et al. *Mon. Not. Roy. Astron. Soc.* **249** 567 (1992)
101. Lyubarsky Yu E, Postnov K A, Prokhorov M E *Mon. Not. Roy. Astron. Soc.* **266** 583 (1994)
102. Antokhina E A, Cherepashchuk A M *Astron. Zh.* **64** 562 (1987) [*Sov. Astron.* **31** 295 (1987)]
103. Pustylnik I B, Einasto L *Astrophys. Space Sci.* **105** 259 (1984)
104. Cherepashchuk A M, Khruzina T S *Astron. Zh.* **58** 1226 (1981) [*Sov. Astron.* **25** 697 (1981)]
105. Balog N I et al. *Astron. Zh.* **60** 534 (1983) [*Sov. Astron.* **27** 310 (1983)]
106. Hulse R A, Taylor J H *Astrophys. J. Lett. Ed.* **195** L51 (1975)
107. Taylor J H, Weisberg J M *Astrophys. J.* **254** 1 (1982)
108. Krat V A *Kurs astrofiziki i zvezdnoi astronomii* (Course of Astrophysics and Stellar Astronomy) (Ed. A A Mikhailov) (Moscow: Fizmatgiz , 1962) p. 87
109. Hutchings J B *Publ. Dom. Astrophys. Obs.* **14** 59 (1972)
110. Wilson R E, Sofia S *Astrophys. J.* **203** 182 (1976)
111. Milgrom M *Astrophys. J.* **206** 869 (1976)
112. Milgrom M, Katz J I *Astrophys. J.* **205** 545 (1976)
113. Milgrom M *Astron. Astrophys.* **54** 725 (1977)
114. Milgrom M, Salpeter E E *Astrophys. J.* **196** 583 (1975)
115. Antokhina E A, Cherepashchuk A M *Astron. Zh.* **71** 420 (1994)
116. Kurucz R L *Astrophys. J. Suppl.* **40** 1 (1979)
117. Batten A *Binary and Multiple Systems of Stars* (Oxford, New York: Pergamon Press, 1973) [Translated into Russian (Moscow: Mir, 1976) p. 200]
118. Casares J, Charles P A, Marsh T R *Mon. Not. Roy. Astron. Soc.* **277** L45 (1995)
119. Rappaport S A, Joss P C, in *Accretion Driven Stellar X-ray Sources* (Eds W H G Lewin, E P J Van den Heuvel) (Cambridge: Cambridge Univ. Press., 1984) p. 1
120. Khruzina T S *Astron. Zh.* **62** 356 (1985) [*Sov. Astron.* **29** 205 (1985)]
121. Paczynski B *Astrophys. J.* **216** 822 (1977)
122. Paszynski B *Astron. Astrophys.* **34** 161 (1974)
123. Allen K U *Astrofizicheskie velichiny* (Astrophysical Quantities) (Moscow: Mir, 1977) p. 279
124. Wade R A, Horne K *Astrophys. J.* **324** 411 (1988)
125. Martin A S et al. *Mon. Not. Roy. Astron. Soc.* **274** L46 (1995)
126. Webster B L, Murdin P *Nature* (London) **235** 37 (1972)
127. Bolton C T *Astrophys. J.* **200** 269 (1975)
128. Oda M *Space Sci. Rev.* **20** 757 (1977)
129. Maejima Y et al. *Astrophys. J.* **285** 712 (1984)

130. Chagelishvili G D, Lominadze J G, Rogava A D, in *Adv. Space Res. The Physics of Compact Objects* Vol. 8 (Eds N E White, L G Filipov) (Oxford–Toronto: Pergamon Press, 1988) p. 211
131. Chagelishvili G D, Chanishvili R G, Lominadze J G, in *Adv. Space Res. The Physics of Compact Objects* Vol. 8 (Eds N E White, L G Filipov) (Oxford–Toronto: Pergamon Press, 1988) p. 217
132. Chagelishvili G D, Lominadze J G, Rogava A D *Astrophys. J.* **347** 1100 (1989)
133. Rotschild R E et al. *Astrophys. J.* **189** L13 (1974)
134. Syunyaev R A *Astron. Zh.* **49** 1153 (1972) [*Sov. Astron.* **16** 941 (1973)]
135. Avni Y, Bahcall J *Astrophys. J.* **197** 675 (1975)
136. Bochkarev N G, Karitskaja E A, Shakura N I *Pis'ma Astron. Zh.* **1** 12 (1975)
137. Margon B, Bowyer S, Stone R P S *Astrophys. J. Lett. Ed.* **185** L113 (1973)
138. Bahcall J N et al. *Astrophys. J. Lett. Ed.* **189** L17 (1974)
139. Aslanov A A, Cherepashchuk A M *Astron. Zh.* **59** 290 (1982) [*Sov. Astron.* **26** 177 (1982)]
140. Kemp J C et al. *Astrophys. J. Lett. Ed.* **271** L65 (1983)
141. Cowley A P et al. *Astrophys. J.* **272** 118 (1983)
142. Khruzina T S, Cherepashchuk A M *Astron. Zh.* **61** 299 (1984) [*Sov. Astron.* **28** 173 (1984)]
143. Bochkarv N G et al. *Astron. Zh.* **65** 778 (1988) [*Sov. Astron.* **32** 405 (1988)]
144. Cowley A P et al. *Astrophys. J.* **381** 526 (1991)
145. Paczynski B *Astrophys. J. Lett. Ed.* **273** L81 (1983)
146. McClintock J E, Remillard R A *Astrophys. J.* **308** 110 (1986)
147. Kundt W *Astron. Astrophys.* **80** L7 (1979)
148. Marsh T R, Robinson E L, Wood J H *Mon. Not. Roy. Astron. Soc.* **266** 137 (1994)
149. Martin E L et al. *Astrophys. J.* **435** 791 (1994)
150. Khruzina T C et al. *Adv. Space Res.* **8** 237 (1988)
151. Shahbaz T, Naylor T, Charles P A *Mon. Not. Roy. Astron. Soc.* **268** 756 (1994)
152. Haswell C A et al. *Astrophys. J.* **411** 802 (1993)
153. Bartolini C et al. *IAU Colloq. № 129, Structure and Emission Properties of Accretion Disks* (Eds C Bertout et al.) (Paris: Edition Frontieres, 1991) p. 373
154. Casares J, Charles P A, Naylor T *Nature* **355** 614 (1992)
155. Martin E L et al. *Nature* **358** 129 (1992)
156. Casares J et al. *Mon. Not. Roy. Astron. Soc.* **265** 834 (1993)
157. Antokhina E A et al. *Astron. Zh.* **70** 804 (1993)
158. Wagner R M et al. *Astrophys. J.* **401** L97 (1992)
159. Shahbaz T et al. *Mon. Not. Roy. Astron. Soc.* **271** L10 (1994)
160. Casares J, Charles P A *Mon. Not. Roy. Astron. Soc.* **271** L5 (1994)
161. Lund N, Brandt S *IAU Circ.* № 5161 (1991)
162. Sunyaev R A *IAU Circ.* № 5179 (1991)
163. Makino F, Ginga Teem *IAU Circ.* № 5161 (1991)
164. West R M, Della Valle M, Jarvis B *IAU Circ.* № 5165 (1991)
165. Della Valle M, Jarvis B J, West R M *Astron. Astrophys.* **247** L33 (1991)
166. Remillard R A, McClintock J E, Bailyn C D *Astrophys. J.* **399** L145 (1992)
167. Orosz J A et al. *Bull. Amer. Astron. Soc.* **185** (102.02) 12 (1994)
168. Tsumeni H, Kitamoto S, Roussel-Dupre D *Astrophys. J.* **337** L81 (1989)
169. Wagner R M et al. *Int. Astron. Union Circ.* (4600) 1 (1988)
170. Charles P A et al. *Int. Astron. Union Circ.* (4609) 1 (1988)
171. Chevalier C, Ilovaisky S A *Astron. Astrophys.* **269** 301 (1993)
172. Bailyn C D et al. *Nature* (London) **378** 157 (1995)
173. Remillard R A et al. *Astrophys. J.* **459** 226 (1996)
174. Paciesas W S *IAU Circ.* № 5580 (1992)
175. Wagner R M et al. *IAU Circ.* № 5589 (1992)
176. Sunyaev R et al. *Astron. Astrophys.* **280** L1 (1993)
177. Chevalier C, Ilovaisky S A *Astron. Astrophys.* **297** 103 (1995)
178. Zhao P et al. *IAU Circ.* № 6072 (1994)
179. Chevalier C, Ilovaisky S A *IAU Circ.* № 5974 (1994)
180. Orosz J A, Bailyn C D *Astrophys. J.* **446** L59 (1995)
181. Casares J et al. *Mon. Not. Roy. Astron. Soc.* **276** L35 (1995)
182. Hutchings J B et al. *Astron. J.* **94** 340 (1987)
183. Tutukov A V, Fedorova A V *Astron. Zh.* **66** 1172 (1989)
184. Antokhina E A, Seifina E V, Cherepashchuk A M *Astron. Zh.* **69** 282 (1992)
185. Crampton D, Hutchings J B *Astrophys. J.* **251** 604 (1981)
186. Fabrika S N, Bychkova L V *Astron. Astrophys.* **240** L5 (1990)
187. D'Odorico S et al. *Nature* **353** 329 (1991)
188. Drissen L et al. *Astrophys. J.* **304** 188 (1986)
189. Van Kerkwijk M H et al. *Nature* **355** 703 (1992)
190. Cherepashchuk A M, Moffat A F J *Astrophys. J.* **424** L53 (1994)
191. Samimi J et al. *Nature* (London) **278** 434 (1978)
192. White N E, Marshall F E *Astrophys. J.* **281** 354 (1984)
193. Crampton D, Cowley A P, Hutchings J B *Astrophys. J. Lett. Ed.* **235** L131 (1980)
194. Ford H C et al. *Astrophys. J.* **435** L27 (1994)
195. Miyoshi M et al. *Nature* (London) **373** 127 (1995)
196. Wolszczan A *Nature* (London) **350** 688 (1991)
197. Ryba M, Taylor J H *Astrophys. J.* **371** 739 (1991)
198. Phinney E S *Astrophys. J.* **380** L17 (1991)
199. Martynov D Ya *Usp. Fiz. Nauk* **108** 701 (1973) [*Sov. Phys. Usp.* **15** 786 (1973)]
200. Hameury J M, King A R, Lasota J-P *Astron. Astrophys.* **162** 71 (1986)
201. Hameury J M, King A R, Lasota J-P *Astrophys. J.* **353** 585 (1990)
202. Goutikakis C, Hameury J M *Astron. Astrophys.* **271** 118 (1993)
203. Narayan R, McClintock J E, Insu Yi *Astrophys. J.* **457** 821 (1996)
204. Brandt W N, Podsiadlowski P, Sigurdsson S *Mon. Not. Roy. Astron. Soc.* **277** L35 (1995)
205. Thorne K S, Zytkow A N *Astrophys. J.* **212** 832 (1977)
206. Podsiadlowski P, Cannon R C, Rees M J *Mon. Not. Roy. Astron. Soc.* **274** 485 (1995)
207. Eggleton P P, Verbunt F *Mon. Not. Roy. Astron. Soc.* **220** 13P (1986)
208. De Kool M, Van der Heuvel E P J, Pylyser E *Astron. Astrophys.* **183** 47 (1987)
209. Shore S, Livio M, Van der Heuvel E P J *Interacting Binaries* (Berlin, Budapest: Springer-Verlag, 1994)
210. Masevich A G, Tutukov A V *Evolyutsiya zvezd: teorija i nablyudeniya* (Stellar Evolution: Theory and Observations) (Moscow: Nauka, 1988) p. 195
211. Bisnovatyi-Kogan G S *Fizicheskie voprosy teorii zvezdnoi evolyutsii* (Physical Problems of Stellar Evolution Theory) (Moscow: Nauka, 1989) p. 273
212. Iben I J, Tutukov A V, Yungelson L R *Astrophys. J. Suppl.* **100** 217, 233 (1995)